

**DESIGN AND SYNTHESIS OF A BODIPY BASED  
PROBE FOR MERCURY IONS**

**A Thesis Submitted to  
The Graduate School of Engineering and Sciences of  
İzmir Institute of Technology  
in Partial Fulfillment of the Requirements for the Degree of  
MASTER OF SCIENCE  
in Chemistry**

**by  
Büşra Buse TÛTÛNCÛ**

**December 2021**

**İZMİR**

## ACKNOWLEDGEMENTS

Many people have supported me during my studies. Firstly, I would like to express my appreciation to Prof. Dr. Mustafa EMRULLAHOĞLU for allowing me to work in this laboratory, for his help, attention, and patience. This thesis could not have been written without his supervision, and it was an honor for me to work with him.

I am very grateful to the members of Emrullahođlu Research Group; Miray CEBECİ, Ezgi VURAL, Beraat Umur KAYA, Ahmet EREN, and especially Suay DARTAR for her endless tolerance and guidance during my studies. I would like to extend special thanks to Miray CEBECİ for her support and long-lasting friendship. I feel blessed to have had a sister like her by my side for the last seven years.

Moreover, I would like to thank Hazal TOSUN, Sümeyra Çiğdem SÖZER, Bilgesu ERDOĞAN, Pınar ÖZTÜRK, Ece TOPCU, Selen DAL, İlyas Yasin ÇİFTÇİ, Onur TEKİN and Turgut UĞUR for their never-ending friendship and everlasting encouragement.

I would like to thank the TUBITAK for its fellowship support (118Z418) during my master's degree studies.

Also, special thanks to my committee members, Prof. Dr. Hasan ŞAHİN and Asst. Prof. Dr. Nuriye Tuna SUBAŞI for participating and reviewing my work.

I am truly thankful to my family, Göksel TÛTÛNCÛ, Selma TÛTÛNCÛ, and my beloved brother Emir TÛTÛNCÛ. Whenever I got desperate, they always provided all the moral support and love. I love them with all my heart.

Finally, I would like to thank Tuna DURAN for believing in me and loving me unconditionally.

## **ABSTRACT**

### **DESIGN AND SYNTHESIS OF A BODIPY BASED PROBE FOR MERCURY IONS**

The detection of heavy metal ions in living systems and aqueous environments has attracted significant attention in recent years, especially the detection of mercury, one of the most toxic heavy metals on Earth. To reduce mercury's lethal effects on the human body, animals, and marine life trace amounts of mercury species can be detected by using classical spectroscopic techniques for example atomic absorption and emission spectroscopy, high-performance liquid chromatography, and inductively coupled plasma mass spectrometry. However, because those techniques are time-consuming and expensive, fluorescence analysis, which offers high selectivity and sensitivity, has emerged as a suitable alternative for detecting mercury species.

In the work presented here, a new BODIPY -based fluorescent probe functionalised with a phenylhydrazine unit was designed and synthesised for the selective and sensitive detection of mercury species. The probe's detection limit was determined to be 29 nM, and the probe could detect mercury species in living cells without any changes in cell morphology.

# ÖZET

## CİVA İYONLARI İÇİN BODIPY BAZLI ALGILAYICININ TASARIMI VE SENTEZİ

Canlı sistemlerde ve sulu ortamlarda ağır metal iyonlarının tespiti, özellikle dünya üzerindeki en zehirli ağır metallere biri olan cıvanın tespiti, son yıllarda büyük ilgi görmüştür. Cıvanın insan vücudu, hayvanlar ve deniz yaşamı üzerindeki öldürücü etkilerini azaltmak için eser miktarda cıva türü, atomik absorpsiyon ve emisyon spektroskopisi, yüksek performanslı sıvı kromatografisi ve endüktif olarak eşleştirilmiş plazma kütle spektrometrisi gibi klasik spektroskopik teknikler kullanılarak tespit edilebilir. Ancak, bu tekniklerin zaman alıcı ve pahalı olması nedeniyle, yüksek seçicilik ve hassasiyet sunan floresan analizi, cıva türlerinin tespiti için uygun bir alternatif olarak ortaya çıkmıştır.

Burada sunulan çalışmada, cıva türlerinin seçici ve hassas tespiti için bir fenilhidrazin ünitesi ile işlevselleştirilmiş yeni bir BODIPY bazlı floresan probu tasarlanmış ve sentezlenmiştir. Probenin tespit limiti 29 nM olarak belirlenmiştir ve prob, hücre morfolojisinde herhangi bir değişiklik olmaksızın canlı hücrelerdeki cıva türlerini tespit edebilmiştir.

# TABLE OF CONTENTS

LIST OF FIGURES .....	vii
LIST OF ABBREVIATIONS.....	x
CHAPTER 1_ INTRODUCTION .....	1
1.1. An Overview .....	1
1.2. BODIPY Fluorophore.....	2
1.3. Literature Studies .....	6
CHAPTER 2_ EXPERIMENTAL STUDY .....	12
2.1. General Methods.....	12
2.2. Determination of Quantum Yields.....	12
2.3. Synthesis Section .....	13
2.3.1. Synthesis of BODIPY.....	13
2.3.2. Synthesis of IODO-BODIPY .....	14
2.3.3. Synthesis of BDP-PRP .....	15
2.3.4. Synthesis of BDP-AL .....	15
2.3.5. Synthesis of BDP-BUS.....	16
2.3.6. Synthesis of BDP-PYRZL.....	17
CHAPTER 3. RESULTS AND DISCUSSION.....	18
CHAPTER 4. CONCLUSION .....	24

REFERENCES .....	25
------------------	----

## APPENDICES

APPENDIX A. $^1\text{H}$ -NMR AND $^{13}\text{C}$ -NMR SPECTRA OF COMPOUNDS .....	29
-----------------------------------------------------------------------------------	----

APPENDIX B. MASS SPECTRA OF COMPOUNDS .....	33
---------------------------------------------	----

# LIST OF FIGURES

<b><u>Figure</u></b>	<b><u>Page</u></b>
Figure 1.1. First synthesis of a boron dipyrin dye by Treibs and Kreuzer (Source: Treibs and Kreuzer, 1968) .....	2
Figure 1.2. IUPAC numbering system of a boron dipyrin compound .....	3
Figure 1.3. Acid catalyzed condensation of aromatic aldehydes with pyrroles .....	3
Figure 1.4. Synthesis of BODIPY dyes with the acylation of pyrrole followed by condensation and complexation .....	4
Figure 1.5. The new approach described by Wu and Burgess (Source: Wu et al., 2008)	4
Figure 1.6. BODIPY structures with different absorption and emission wavelengths (Source: Ni and Wu, 2014) .....	5
Figure 1.7. Reaction and coordination based approaches (Source: Patil et al., 2012).....	5
Figure 1.8. First developed Hg <sup>2+</sup> chemodosimeter (Source: Chae et al., 1992) .....	6
Figure 1.9. Proposed Hg <sup>2+</sup> -Promoted Ring Opening of Spirolactam and Intramolecular Guanylation (Source: Wu et al., 2007) .....	7
Figure 1.10. First example of Hg <sup>2+</sup> sensor bearing alkyne moiety (Source: Song et al., 2008) .....	7
Figure 1.11. The proposed reaction mechanism of Rhodamine based probe with Hg <sup>2+</sup> (Source: Lin et al., 2010)) .....	8
Figure 1.12. Ratiometric fluorescent sensing of Hg <sup>2+</sup> and Au <sup>3+</sup> (Source: Dong et al., 2010) .....	8
Figure 1.13. Hg (II)-mediated propargyl amide to oxazole transformation (Source: Lee and Kim, 2011) .....	9
Figure 1.14. Proposed Mechanisms of Hg (II)-Mediated Intramolecular Cyclization (Source: Atta et al., 2013) .....	9
Figure 1.15. The proposed sensing mechanism of the probe towards Hg <sup>2+</sup> (Source: Kaur and Choi, 2014) .....	10
Figure 1.16. Proposed mechanism of BODIPY based probe towards to gold and mercury species (Source: Üçüncü et al., 2015) .....	11
Figure 1.17. Detection mechanism of the probe (Source: Duan et al., 2017).....	11
Figure 2.1. Synthesis pathway of BDP-BUS and BDP-PYRZL. ....	13

<u>Figure</u>	<u>Page</u>
Figure 2.2. 5,5-difluoro-1,3,7,9-tetramethyl-10-phenyl-5H-4 $\lambda^4$ ,5 $\lambda^4$ -dipyrrolo [1,2-c:2',1'-f][1,3,2]diazaborinine .....	14
Figure 2.3. 5,5-difluoro-2-iodo-1,3,7,9-tetramethyl-10-phenyl-5H-5 $\lambda^4$ ,6 $\lambda^4$ -dipyrrolo [1,2-c:2',1'-f][1,3,2]diazaborinine .....	14
Figure 2.4. 3-(5,5-difluoro-1,3,7,9-tetramethyl-10-phenyl-5H-5 $\lambda^4$ ,6 $\lambda^4$ -dipyrrolo [1,2-c:2',1'-f][1,3,2]diazaborinin-2-yl)prop-2-yn-1-ol .....	15
Figure 2.5. 3-(5,5-difluoro-1,3,7,9-tetramethyl-10-phenyl-5H-5 $\lambda^4$ ,6 $\lambda^4$ -dipyrrolo [1,2-c:2',1'-f][1,3,2]diazaborinin-2-yl)propiolaldehyde .....	16
Figure 2.6. (Z) -5,5- difluoro-1,3,7,9-tetramethyl-10-phenyl-2- (3- (2 phenylhydrazono) prop-1-yn-1-yl)- 5H-5 $\lambda^4$ ,6 $\lambda^4$ -dipyrrolo [1,2-c:2',1'-f][1,3,2]diazaborinine ...	17
Figure 2.7. 5,5-difluoro-1,3,7,9-tetramethyl-10-phenyl-2-(1-phenyl-1H-pyrazol-5-yl)- 5H-5 $\lambda^4$ ,6 $\lambda^4$ -dipyrrolo[1,2-c:2',1'-f][1,3,2]diazaborinine .....	17
Figure 3.1. Effect of pH on the interaction of BDP-BUS (10.0 $\mu$ M) with 10 equiv. $Hg^{2+}$ in ACN/PBS buffer solution (3:7, v/v, pH = 7.4). ( $\lambda_{ex}$ = 480 nm, $\lambda_{em}$ = 530 nm at 25 $^{\circ}$ C) .....	18
Figure 3.2. Absorption (a) and fluorescence (b) spectra of BDP-BUS (10 $\mu$ M) in CH <sub>3</sub> CN/PBS buffer solution (3:7, v/v, pH = 7.4) ( $\lambda_{ex}$ = 480 nm).....	19
Figure 3.3. Time dependent fluorescence changes of BDP-BUS (10.0 $\mu$ M) with 10 equiv. $Hg^{2+}$ in CH <sub>3</sub> CN/PBS buffer solution (3:7, v/v, pH = 7.4). ( $\lambda_{ex}$ = 480 nm, $\lambda_{em}$ = 530 nm at 25 $^{\circ}$ C) within 10 min.....	20
Figure 3.4. Fluorescence spectra of BDP-BUS (10 $\mu$ M) in CH <sub>3</sub> CN/PBS buffer solution (3:7, v/v, pH = 7.4) in the presence of different concentrations of $Hg^{2+}$ (0–30 equiv). Inset: Calibration curve. ( $\lambda_{ex}$ = 480 nm at 25 $^{\circ}$ C).. .....	20
Figure 3.5. a) Fluorescence intensity of BDP-BUS (10 $\mu$ M) in CH <sub>3</sub> CN/PBS buffer (3:7, v/v, pH= 7.4) with representative cations (100 $\mu$ M) b) fluorescence responses of BDP-BUS to various metal ions including $Hg^{2+}$ , $Au^{3+}$ $Pd^{2+}$ , $Cu^{2+}$ , $Ag^{+}$ , $Li^{+}$ , $Mn^{2+}$ , $Ca^{2+}$ , $Mg^{2+}$ , $Ba^{2+}$ , $Au^{+}$ , $Cr^{2+}$ , $Mg^{2+}$ , $Fe^{3+}$ , $Ni^{2+}$ , $Cu^{2+}$ , $Zn^{2+}$ , $Cd^{2+}$ and $Al^{3+}$ .....	21
Figure 3.6. Fluorescence changes of BU-49 (10.0 $\mu$ M) upon addition of $Hg^{2+}$ (0.1 to 1 equiv.) in ACN/PBS buffer solution (3:7, v/v, pH = 7.4). ( $\lambda_{ex}$ = 480 nm, $\lambda_{em}$ = 530 nm at 25 $^{\circ}$ C).....	22



<b><u>Figure</u></b>	<b><u>Page</u></b>
Figure 3.7. Cyclization reaction of BDP-BUS .....	23
Figure 3.8. Fluorescence images of human lung adenocarcinoma (A549) cells .....	23

## LIST OF ABBREVIATIONS

<b>BODIPY</b>	4, 4-difluoro-4-bora-3a, 4a-diaza-s-indacene
<b>THF</b>	Tetrahydrofuran
<b>DDQ</b>	2,3-Dichloro-5,6-dicyano-1,4-benzoquinone
<b>POCl<sub>3</sub></b>	Phosphorous oxychloride
<b>DCM</b>	Dichloromethane
<b>BF<sub>3</sub>.Et<sub>2</sub>O</b>	Boron trifluoride diethyl etherate
<b>ACN</b>	Acetonitrile
<b>PBS</b>	Phosphate-Buffered Saline
<b>CDCl<sub>3</sub></b>	Deutero Chloroform
<b>NMR</b>	Nuclear Magnetic Resonance
<b>MnO<sub>2</sub></b>	Manganese Oxide
<b>NIS</b>	N- Iodosuccinamide
<b>MeOH</b>	Methanol
<b>EtOH</b>	Ethanol
<b>DAPI</b>	4',6-diamidino-2-phenylindole

# CHAPTER 1

## INTRODUCTION

### 1.1. An Overview

Environmental pollution in air, soil, and water due to contamination with heavy metals is a vital problem that affects human life, marine life, and animals in general. Of all heavy metal, mercury is one of the most toxic because it accumulates in the body even at low concentrations, affects the central nervous system due to the thiophilic nature of proteins and enzymes, and can consequently cause cancer, skin disorders, and kidney failure, among other critical conditions. Therefore, designing selective, sensitive methods of detecting mercury in living cells is crucial.

To date, heavy metal ions have been detected by analytical methods such as atomic absorption spectroscopy, high-performance liquid chromatography, inductively coupled plasma mass spectrometry, and atomic fluorescence spectrometry. Despite the excellent performance of those techniques, their drawbacks include complicated sample preparation, expensive instrumentation, and lack of portability. For those reasons, fluorescence-based probes are highly preferred due to their high selectivity, high sensitivity, simplicity, low cost, and low detection limits.

Every fluorescent probe includes two units, a fluorophore unit and a receptor unit, the latter of which is an analyte-specific unit that determines the behaviour of a targeted analyte based on reaction or coordination chemistry. Highly selective, usually irreversible reactions that occur with the appearance of targeted molecules can be determined with a chemodosimeter. By contrast, chemosensors operate based on coordination, and reactions in molecules with the target analyte are reversible.

Numerous organic dye molecules are used in fluorescence-based probe strategies, including rhodamine derivatives, fluorescein, coumarin, and boron dipyrin (BODIPY) derivatives. Owing to their unique properties, BODIPY fluorophores have attracted considerable attention in recent years.

In the work presented here, we took advantage of the alkynophilic nature of  $\text{Hg}^{2+}$  to design and synthesise a new BODIPY derivative functionalised with a phenylhydrazine moiety that is highly selective and sensitive to  $\text{Hg}^{2+}$  ions over relevant competing metal ions. We also investigated the derivative's potential for tracking  $\text{Hg}^{2+}$  ions in living cells.

## 1.2. BODIPY Fluorophore

BODIPY (4,4-difluoro-4-bora-3a, 4a-diaza-s-indacene) fluorophore was first noticed by Treibs and Kreuzer in 1968 (Treibs and Kreuzer, 1968). They discovered that the acylation of 2,4-dimethylpyrrole with acetic anhydride and boron trifluoride formed a highly fluorescent compound.

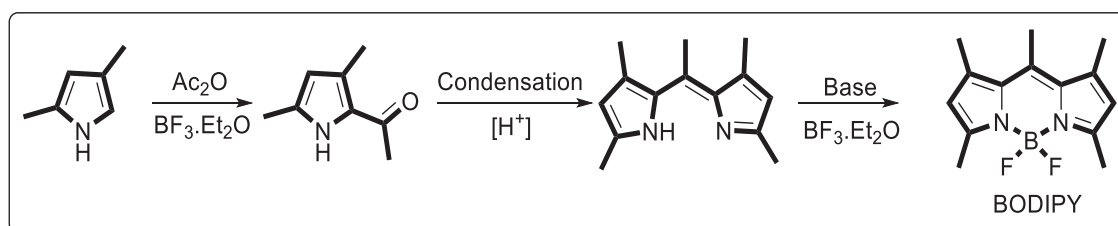


Figure 1.1. First synthesis of a BODIPY dye by Treibs and Kreuzer  
(Source: Treibs and Kreuzer, 1968)

BODIPY dyes have remarkable properties, including excellent stability, high fluorescence quantum yields, large molar absorption coefficients, narrow absorption and emission bands in the visible wavelength range, and good solubility. Those features distinguish BODIPY among fluorescent dyes as candidates for use in biological systems. (Loudet et al., 2007; Ulrich et al., 2008; Leen et al., 2011)

The IUPAC's numbering system for a BODIPY (i.e. boron dipyrin) compound is shown in Figure 1.2. Although BODIPY dyes are numbered differently from their precursors, the  $\alpha$ -,  $\beta$ -, and meso-positions are the same for both. The carbon's position at the centre of the molecule is called the meso-position, the positions adjacent to nitrogen atoms are  $\alpha$ -positions, and the other positions are  $\beta$ -positions.

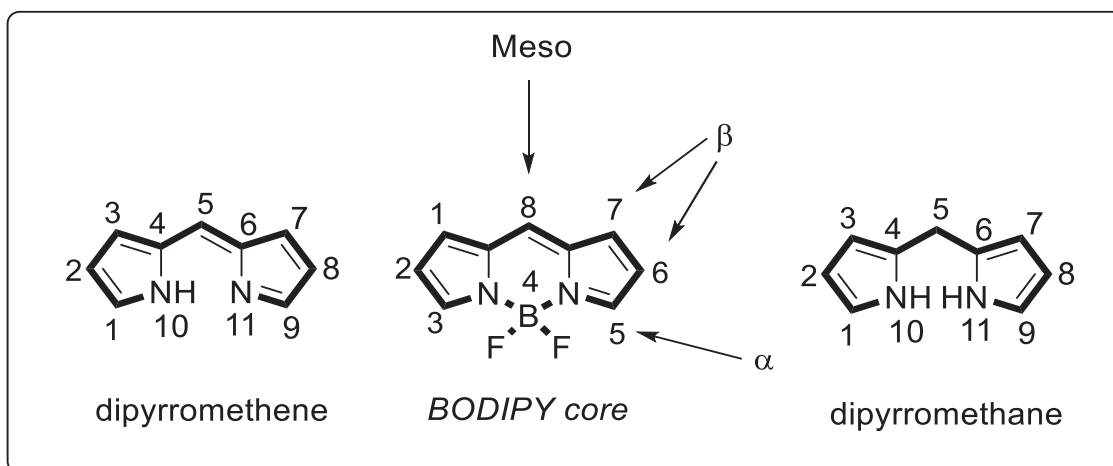


Figure 1.2. IUPAC numbering system of a boron dipyrin compound  
(Source: Wood and Thompson, 2007)

Two methods based on porphyrin chemistry can be used to synthesise the BODIPY structure (Wood et al., 2007). In the first method, an acid-catalysed condensation of pyrrole with an aldehyde yields a dipyrromethane. In that reaction, because the dipyrromethane compound is sensitive to light, air, and acid, it immediately oxidises to dipyrromethene with an oxidant such as 2,3-dichloro-5,6-dicyano-1,4-benzoquinone (DDQ) or the milder 2,3,5,6-tetrachloro-1,4-benzoquinone *p*-chloranil. Once oxidation is complete, dipyrromethene reacts with  $\text{BF}_3 \cdot \text{Et}_2\text{O}$  and a base to produce the BODIPY structure.

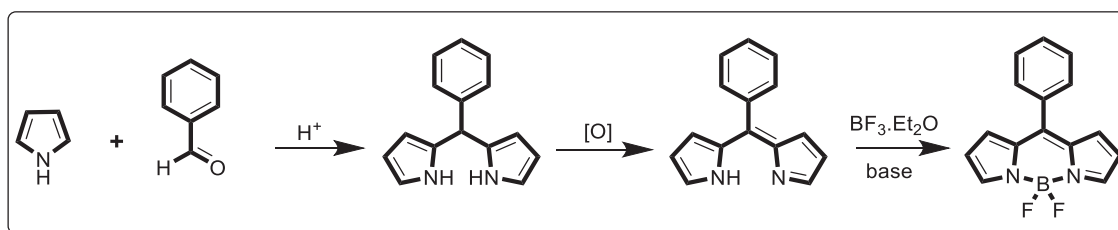


Figure 1.3. Acid catalyzed condensation of aromatic aldehydes with pyrroles  
(Source: Boens et al., 2012)

The second method involves the condensation of pyrrole with an acylium derivative (e.g. an ortho ester, an acid anhydride, or an acid chloride) (Yakubovskiy et al., 2009; Li et al., 2006; Shah et al., 1990). With the reaction between the isolated acyl pyrrole and second pyrrole moiety occurs in an acidic environment, a dipyrin compound is obtained,

and the BODIPY compound materialises with the addition of boron trifluoride etherate and a base.

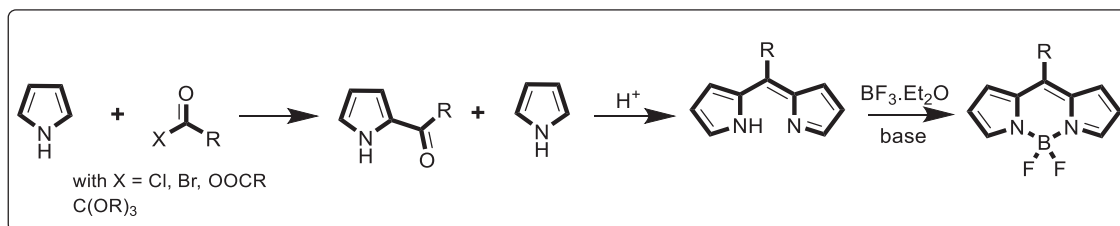


Figure 1.4. Synthesis of BODIPY dyes with the acylation of pyrrole followed by condensation and complexation  
(Source: Boens et al., 2012)

However, in 2008, Wu and Burgess proposed that BODIPY complexes can be obtained without using a second pyrrole equivalent or other condensation reagents. (Wu et al., 2008). Instead, they discovered that phosphorus oxychloride can condense pyrrole-2-carbaldehyde with itself. (Figure 1.5.)

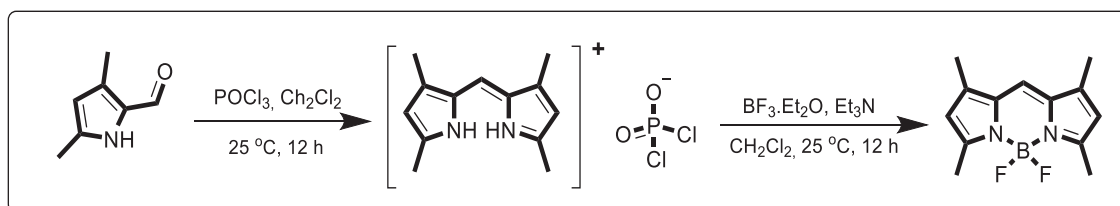


Figure 1.5. The new approach described by Wu and Burgess  
(Source: Wu et al., 2008)

BODIPY dyes absorb and emit at lower wavelengths in the visible range (450- 500 nm) and generally have high quantum yields. Beyond that, the spectroscopic properties of BODIPY can be changed via chemical modification, including by attaching different groups to the proper positions or increasing the conjugation of the BODIPY core, which results in red shifts in its emission wavelength (700 nm) (Chen et al., 2000; Ni et al., 2014).

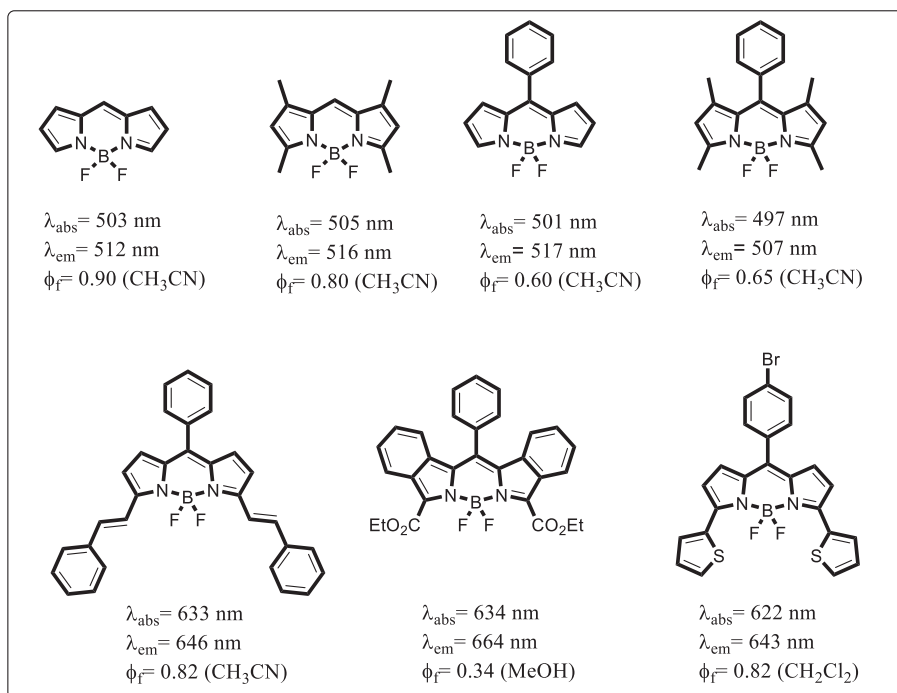


Figure 1.6. BODIPY structures with different absorption and emission wavelengths (Source: Ni and Wu, 2014)

In general, developing fluorescent probes involves two procedures. The first requires using a chemodosimeter such that a fluorophore and a receptor yield a new molecule through a reaction and cause changes in the fluorescence emission. In the second, based on coordination chemistry, the binding of the receptor and metal ion produces a fluorescence signal in which neither the fluorophore nor the receptor are fluorescent before the metal ion is introduced.

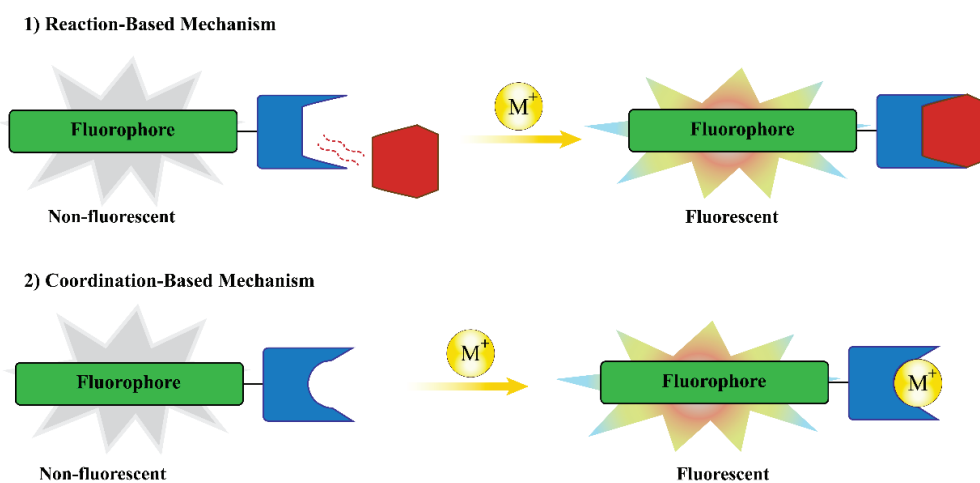


Figure 1.7. Reaction and coordination-based approaches (Source: Patil et al., 2012)

### 1.3. Literature Studies

Since the effects of heavy metals on human health and the environment are recognized, developing fluorescent probes to detect heavy metals has attracted attention over the past decades. Knowing that mercury is one of the most poisonous heavy metals, numerous probes were designed based on a chemodosimetric approach. Furthermore, the high reactivity of mercury ions towards unsaturated bonds has been known and several studies benefited from the strong thiophilic and alkynophilic nature of mercury ions.

In 1992, Czarnik and Chae reported the first mercury selective probe in which an anthracene unit was functionalized with a thioamide group (Chae and Czarnik, 1992). After the isomerization of C=S double bond, thiolate form was produced and as a result, fluorescence emission was quenched via PET mechanism. It is generally known that mercury ions have high affinity to sulphur-based compounds. After adding the mercury ions into the solution of the compound, an irreversible desulfation reaction took place, and the thioamide group was transformed to amide form and as a result, the PET mechanism was blocked. This publication was the first study in which the term chemodosimeter was used. After the discovery of Chae and Czarnik, different fluorescent probes have been developed to detect mercury ions.

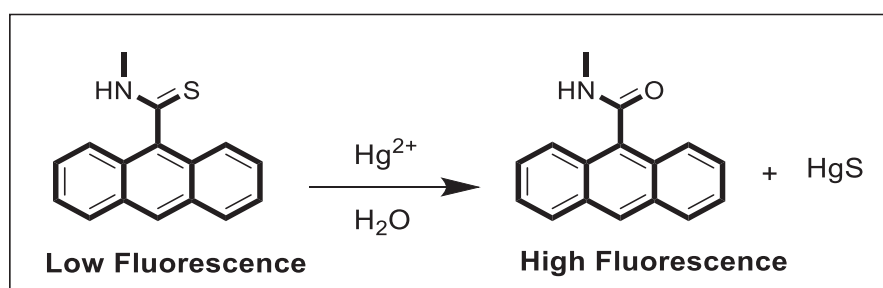


Figure 1.8. First developed  $\text{Hg}^{2+}$  chemodosimeter

(Source: Chae et al., 1992)

In 2007, Wu et al. reported a rhodamine based  $\text{Hg}^{2+}$  chemodosimeter (Wu et al., 2007). They took advantage of the well-known reaction in which thiourea derivatives with amine moiety can be converted into guanidine groups with the addition of the  $\text{Hg}^{2+}$  ion. The probe was nonfluorescent at first. With the promotion of mercury, a



desulfurization reaction took place, and this caused a ring-opening process of spirolactam of rhodamine which resulted in an increment of fluorescent response. Also, a color change from colorless to pink occurred as an outcome of a colorimetric response.

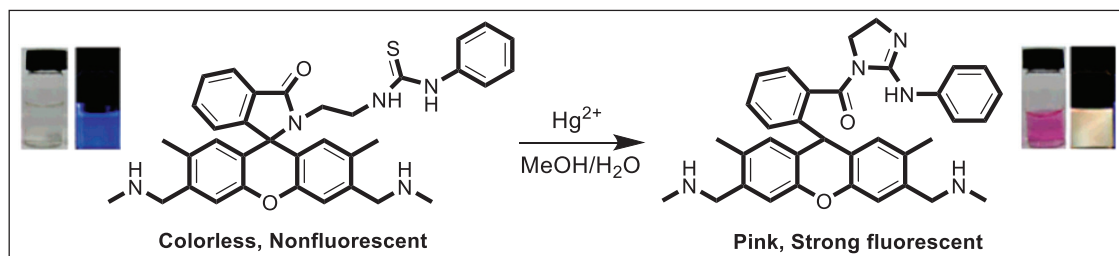


Figure 1.9. Proposed  $\text{Hg}^{2+}$ -Promoted Ring Opening of Spirolactam and Intramolecular Guanylation

(Source: Wu et al., 2007)

In 2008, Koide and co-workers published the first fluorescent probe bearing alkyne moiety to detect mercury ions (Song et al., 2008). They developed a fluorescent probe based on a fluorescein dye that was derivatized from an oxygen atom with an alkyne moiety. At first, the designed molecule was nonfluorescent. The cleavage of the fluorescence-masking alkyne moiety with the addition of  $\text{Hg}^{2+}$  resulted in an increment of fluorescent emission, providing a bright green fluorescent. The probe has enabled the detection of mercury ions in fish and dental samples.

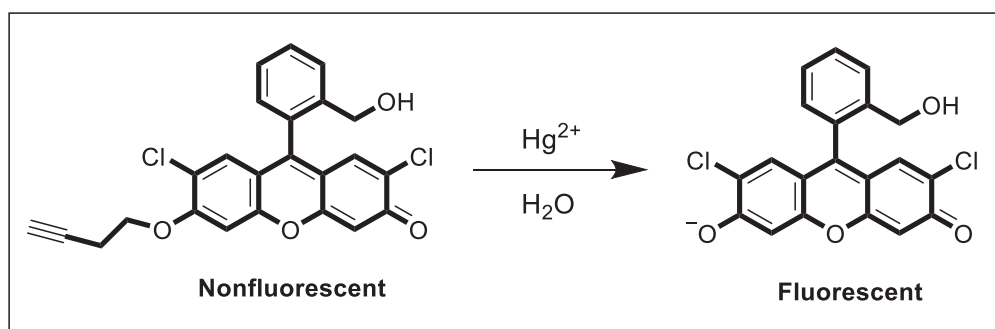


Figure 1.10. First example of  $\text{Hg}^{2+}$  sensor bearing alkyne moiety  
(Source: Song et al., 2008)

At the beginning of 2010, Lin and co-workers were designed a new fluorescent probe bearing both thiol and alkyne moieties in the rhodamine structure for the mercury imaging in living cells (Lin et al., 2010). The interaction of mercury with thiol and alkyne

units in the presence of water enabled the transformation of the rhodamine dye from the non-fluorescent spirocyclic form to the fluorescent opened-ring form.

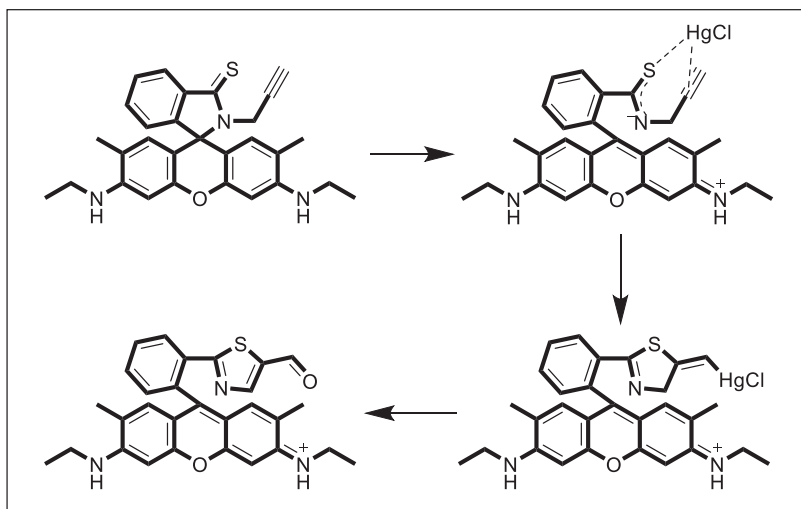


Figure 1.11. The proposed reaction mechanism of Rhodamine based probe with  $\text{Hg}^{2+}$  (Source: Lin et al., 2010)

Later in 2010, a nonsulfur probe based on a 1,8-naphthalimide bearing an alkyne unit was reported for the ratiometric fluorescent sensing for mercury ion in water at neutral pH by Dong et al (Dong et al., 2010). By changing the pH of the environment and the solvent system, they also observed the selectivity of probe towards gold ions. Addition of  $\text{Hg}^{2+}$  caused the change in the fluorescence emission band of probe from 543 to 486 nm.

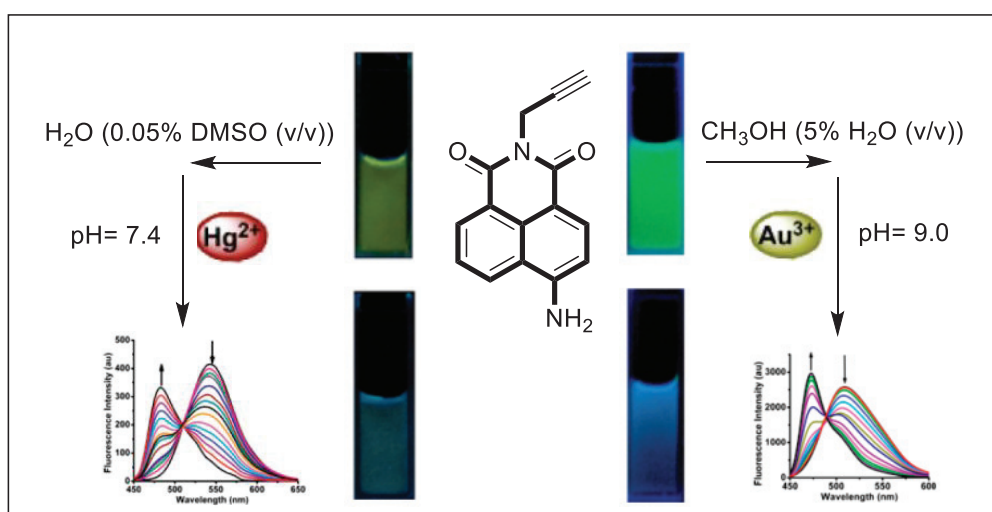


Figure 1.12. Ratiometric fluorescent sensing of  $\text{Hg}^{2+}$  and  $\text{Au}^{3+}$  (Source: Dong et al., 2010)

A ratiometric fluorescent probe functionalized with an alkyne moiety was published by Lee and Kim in 2011 (Lee et al., 2011). They designed an alkyne-tethered coumarin amide. The reaction known as the Kuscheroff reaction took place when mercury ions activated the alkyne unit in the presence of water and afforded an oxazole ring. This caused a significant red shift in the emission from 469 nm to 492 nm.

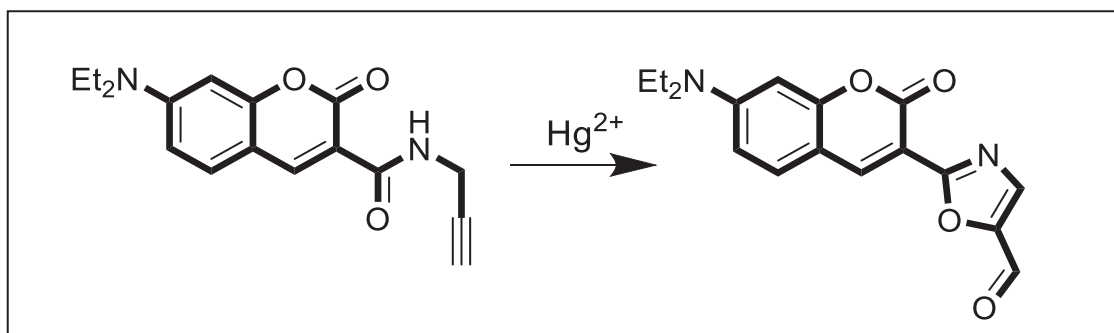


Figure 1.13. Hg (II)-mediated propargyl amide to oxazole transformation  
(Source: Lee and Kim, 2011)

In 2013, Atta and co-workers reported a new fluorescent probe to detect mercury ions in semi aqueous media at ambient temperature. The addition of  $\text{Hg}^{2+}$  to the sensing solution triggered the intramolecular cyclization between phenol and acetylene, providing a form of a benzofuranylmercury chloride. The introduction of  $\text{Hg}^{2+}$  also resulted in a dramatic color change from blue to pale yellow with a very low detection limit of 0.13  $\mu\text{M}$ . No color change was observed upon the addition of other metal ions, except gold ion which is also known for its alkynophilic nature. In the presence of gold ions, the color of the solution was slightly changed.

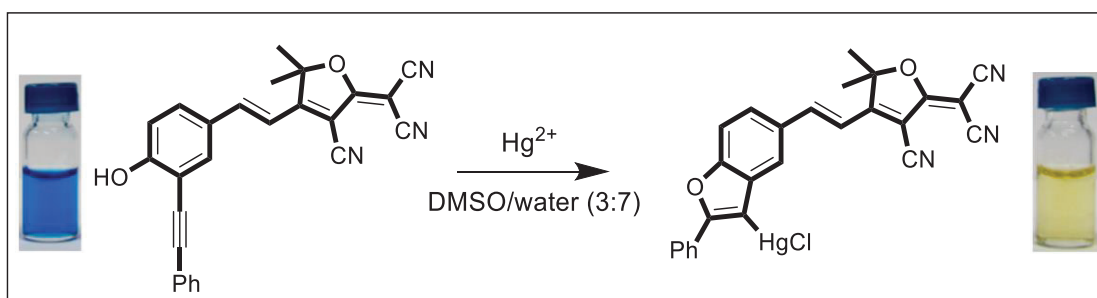


Figure 1.14. Proposed Mechanisms of Hg (II)-Mediated Intramolecular Cyclization  
(Source: Atta et al., 2013)

Another fluorescent probe was reported by Kaur and Choi in 2014 (Kaur and Choi, 2014). Diketopyrrolopyrrole (DPP) dye, which normally used in organic electronic devices but very rare in fluorescent probe, was used as a fluorophore in this research. The probe functionalized with alkynyl and thiophene units was used to detect  $\text{Hg}^{2+}$  and  $\text{Cu}^{2+}$  ions at nanomolar concentrations. In the presence of  $\text{Hg}^{2+}$  in water, the conversion of alkyne to carbonyl took place and a significant color change from pink to blue was observed as a result of a colorimetric response.

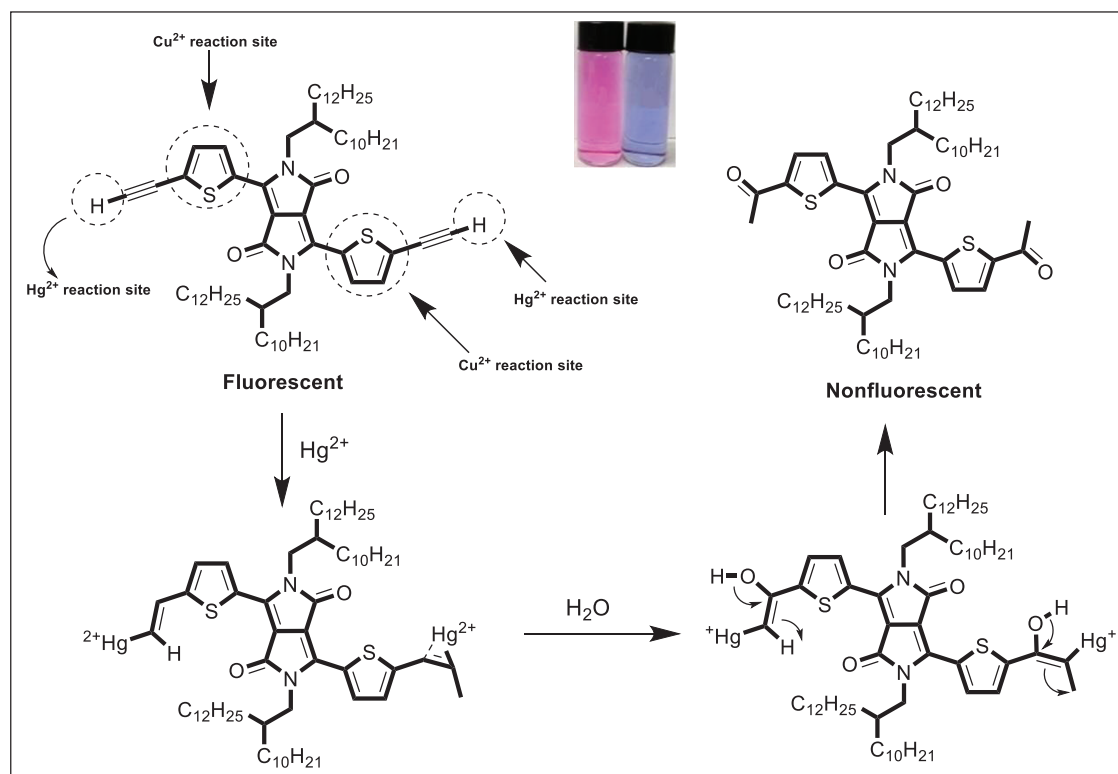


Figure 1.15. The proposed sensing mechanism of the probe towards  $\text{Hg}^{2+}$  (Source: Kaur and Choi, 2014)

In 2015, our group has developed a BODIPY based fluorescent probe for detection of Au (III) and Hg (II) and this work was also benefited the alkynophilic nature of gold and mercury ions. The fluorescent probe showed a ratiometric response towards mercury and gold ions, providing a distinct color change from orange to green. With the extension of non-conjugated BODIPY derivative, a green fluorescence emission was observed.

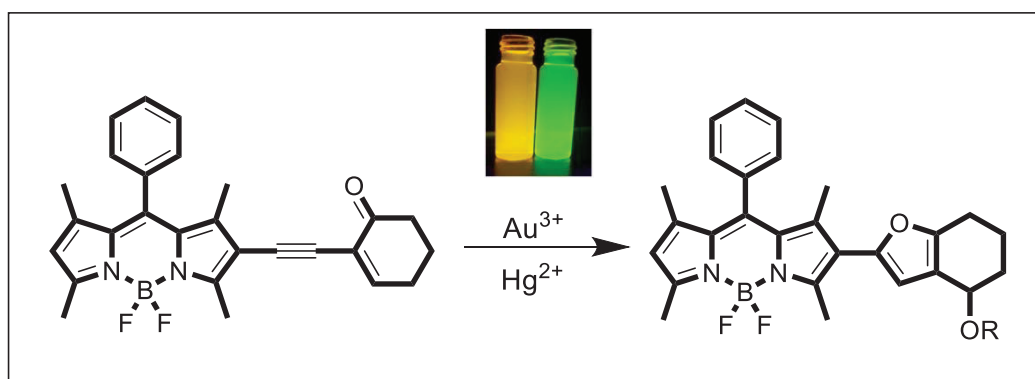


Figure 1.16. Proposed mechanism of BODIPY based probe towards to gold and mercury species

(Source: Üçüncü et al., 2015)

Duan and co-workers presented a novel coumarin based probe, 7-(propargylamino)-4-methyl-2H-chromene-2-one (CNP), bearing alkyne unit that converted into a stable ketone in the presence of mercury ions. (Duan et al., 2017) The probe was nonfluorescent at first due to the ICT process. The detection limit of the probe for the mercury ions was determined in nanomolar range. The sensing probe was designed to be used in environmental samples and on agar gels.

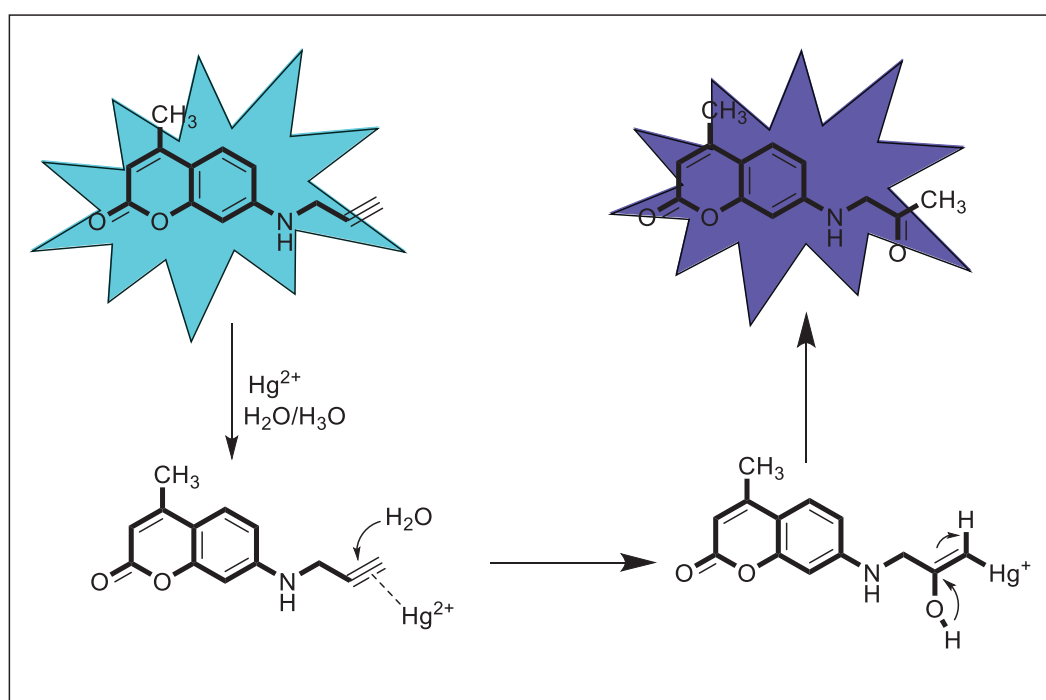


Figure 1.17. Detection mechanism of the probe  
(Source: Duan et al., 2017)

## CHAPTER 2

### EXPERIMENTAL STUDY

#### 2.1. General Methods

All used reagents were obtained from commercial suppliers (Sigma-Aldrich and Merck) and used without any purification.  $^1\text{H}$  NMR and  $^{13}\text{C}$  NMR spectrum were measured on a VNMRJ 400 Nuclear Magnetic Resonance Spectrometer (Varian Medical Systems). UV absorption spectra and Fluorescence emission spectra were obtained using HORIBA Duetta, the two-in-one Fluorescence and absorbance spectrometer. Samples were contained in quartz cuvettes with a path length of 10.0 mm (2.0 mL volume). Upon excitation at 480 nm, the emission spectra were integrated over the range 490 nm to 750 nm. The slit width was 5 nm for both excitation and emission. The pH was recorded by HI-8014 instrument (HANNA). All measurements were regulated at least in triplicate. The fluorescence images were obtained using Zeiss Axio Observer fluorescence microscope.

#### 2.2. Determination of Quantum Yields

Fluorescence quantum yields of **BDP-BUS** and **BDP-PYRZL** were determined by using optically matching solutions of Rhodamine B ( $\Phi_{\text{F}}=0.31$  in water) as a standard. The quantum yield was calculated according to the equation;

$$\Phi_{\text{F(X)}} = \Phi_{\text{F(S)}} (A_{\text{S}}F_{\text{X}}/A_{\text{X}}F_{\text{S}}) (n_{\text{X}}/n_{\text{S}})^2$$

Where  $\Phi_{\text{F}}$  is the fluorescence quantum yield, A is the absorbance at the excitation wavelength, F is the area under the corrected emission curve, and n is the refractive index of the solvents used. Subscripts S and X refer to the standard and to the unknown, respectively.

## 2.3. Synthesis Section

The synthesis pathway for **BDP-BUS** and **BDP-PYRZL** were shown in Figure 2.1. **BODIPY**, **iodo-BODIPY**, **BDP-PRP**, **BDP-AL**, **BDP-BUS** and **BDP-PYRZL** were synthesized by using literature procedures.

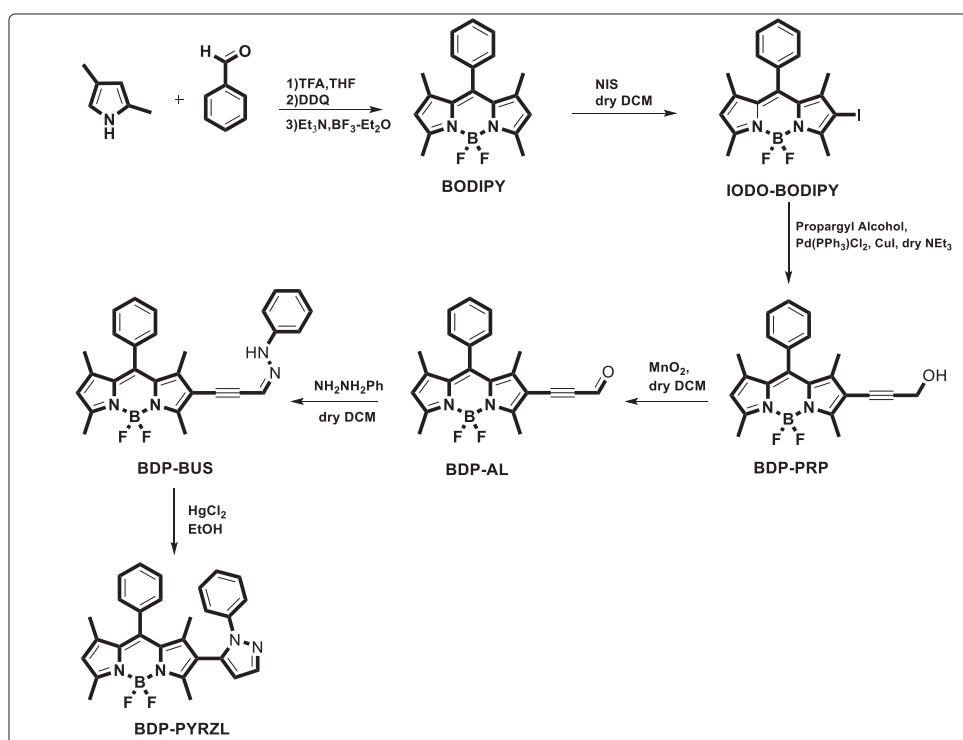


Figure 2.1. Synthesis pathway of **BDP-BUS** and **BDP-PYRZL**

### 2.3.1. Synthesis of BODIPY

**BODIPY** dye was synthesized according to literature procedure (Sauer et al., 2012). To a solution of 2,4-dimethylpyrrole (4 mmol, 411  $\mu$ L) in 25 ml dry THF, benzaldehyde (2 mmol, 200  $\mu$ L) and 60  $\mu$ L trifluoroacetic acid were added under argon atmosphere. After 24 hours, DDQ (2 mmol, 255 mg) was dissolved in 15 ml of dry THF and added to reaction in ice. The resulting mixture was stirred for 4 hours. Then 12 ml of triethylamine was added dropwise in ice and the reaction was stirred further 45 minutes. Finally, 13 ml of BF<sub>3</sub>·Et<sub>2</sub>O was added in ice and the reaction was stirred overnight. At the end of reaction solvent was removed under reduced pressure. Then, extracted with dichloromethane

(3x30 ml) and dried over MgSO<sub>4</sub>. Solvent was evaporated in and the resultant compound purified by column chromatography (%40 yield). <sup>1</sup>H NMR (400 MHz, CDCl<sub>3</sub>) δ: 7.49-7.47 (m, 3H), 7.28-7.26 (m, 2H), 5.98 (s, 2H), 2.55 (s, 6H), 1.37 (s, 6H). <sup>13</sup>C NMR (100 MHz, CDCl<sub>3</sub>) δ: 155.4, 143.2, 141.7, 135.0, 129.1, 128.9, 127.9, 121.29, 15.0, 14.3.

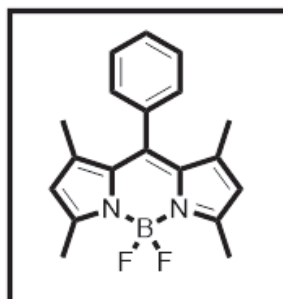


Figure 2.2. 5,5-difluoro-1,3,7,9-tetramethyl-10-phenyl-5H-4λ<sup>4</sup>,5λ<sup>4</sup>-dipyrrolo[1,2-c:2',1'-f][1,3,2]diazaborinine

### 2.3.2. Synthesis of IODO-BODIPY

**IODO-BODIPY** was synthesized by using literature procedure (Wu et al., 2011). N-iodosuccinimide (NIS) (140.0 mg, 0.62 mmol) in anhydrous CH<sub>2</sub>Cl<sub>2</sub> (10 mL) was added dropwise into a solution of BODIPY (200 mg, 0.62 mmol) in CH<sub>2</sub>Cl<sub>2</sub> (20 mL) within ca. 1 h at 0 °C. The reaction mixture was then concentrated under reduced pressure, and the crude product was purified by column chromatography (hexane/EtOAc, 20:1, v/v). The product was collected as a red solid. Yield: 191.7 mg, 68.7%. <sup>1</sup>H NMR (400 MHz, CDCl<sub>3</sub>): δ 7.51- 7.48 (m, 3H), 7.27-7.25 (m, 2H), 6.04 (s, 1H), 2.63 (s, 3H), 2.57 (s, 3H), 1.38 (s, 6H). <sup>13</sup>C NMR (100 MHz, CDCl<sub>3</sub>): δ 157.9, 154.7, 145.3, 143.4, 141.7, 135.0, 132.0, 131.1, 129.8, 129.5, 129.4, 128.0, 122.5, 84.4, 16.8, 16.0, 14.9, 14.7.

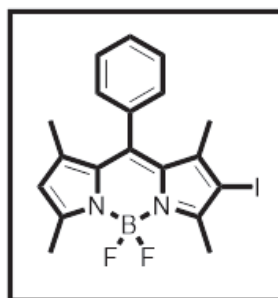


Figure 2.3. 5,5-difluoro-2-iodo-1,3,7,9-tetramethyl-10-phenyl-5H-5λ<sup>4</sup>,6λ<sup>4</sup>-dipyrrolo[1,2-c:2',1'-f][1,3,2]diazaborinine



### 2.3.3 Synthesis of BDP-PRP

**BDP-PRP** was synthesized by using literature procedure (Panteleev et al., 2015). Pd(PPh<sub>3</sub>)<sub>2</sub>Cl<sub>2</sub> (30 mg, 0.042 mmol, 0.1 equiv.) and CuI (16 mg, 0.084 mmol, 0.2 equiv.) were suspended in Et<sub>3</sub>N (4 ml) under argon. Then, IODO-BODIPY (190 mg, 0.42 mmol) was added, followed by propargyl alcohol (182 μL, 175.6 mg, 0.46 mmol, 1.1 equiv), and the reaction was stirred at 40 °C for overnight. After the reaction was over, the extraction was done with the DCM and column chromatography (hexanes:EtOAc 10:1) yielded the title compound as an orange solid. Yield: 80 mg, 50%. <sup>1</sup>H NMR (400 MHz, CDCl<sub>3</sub>) δ 7.53 – 7.46 (m, 3H), 7.30 – 7.22 (m, 2H), 6.03 (s, 1H), 5.30 (s, 1H), 4.49 (d, *J* = 5.0 Hz, 2H), 2.62 (s, 3H), 2.57 (s, 3H), 1.42 (s, 3H), 1.39 (s, 3H). <sup>13</sup>C NMR (101 MHz, CDCl<sub>3</sub>) δ 157.86 (s), 156.32 (s), 144.91 (s), 143.16 (s), 142.18 (s), 134.54 (s), 132.47 (s), 129.20 (d, *J* = 6.7 Hz), 127.75 (s), 122.19 (s), 93.54 (s), 78.24 (s), 77.32 (s), 77.00 (s), 76.68 (s), 51.80 (s), 51.40 (s), 14.75 (s), 14.52 (s), 13.42 (s), 13.02 (s).

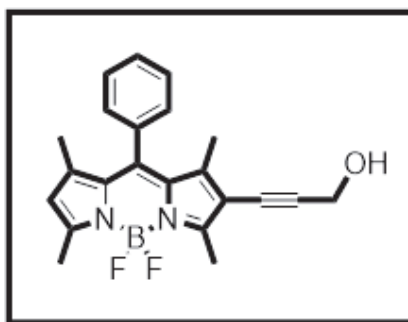


Figure 2.4. 3-(5,5-difluoro-1,3,7,9-tetramethyl-10-phenyl-5H-5λ<sup>4</sup>,6λ<sup>4</sup>-dipyrrolo[1,2-c:2',1'-f][1,3,2]diazaborinin-2-yl)prop-2-yn-1-ol

### 2.3.4 Synthesis of BDP-AL

**BODIPY-AL** was synthesized by using literature procedure (Bobileva et al., 2017). To a solution of BDP-PRP (80 mg, 0.21 mmol) in dry DCM (5 ml) was added MnO<sub>2</sub> (184 mg, 2.11 mmol, 10 equiv.), and the solution was stirred at room temperature for 24 hr. The mixture was filtered through celite with DCM. Then, the filtrate was concentrated and column chromatography was done (hexane:EtOAc, 7:1) to obtain the product (68 mg, 86%) as a yellow solid. <sup>1</sup>H NMR (400 MHz, CDCl<sub>3</sub>) δ 9.37 (d, *J* = 2.4 Hz, 1H), 7.53

(dd,  $J = 4.3, 2.1$  Hz, 3H), 7.28 – 7.25 (m, 2H), 6.13 (s, 1H), 2.68 (s, 3H), 2.61 (s, 3H), 1.48 (s, 3H), 1.43 (s, 3H).  $^{13}\text{C}$  NMR (101 MHz,  $\text{cdcl}_3$ )  $\delta$  176.04 (s), 161.22 (s), 157.18 (s), 147.12 (s), 144.33 (s), 142.69 (s), 133.86 (d,  $J = 19.1$  Hz), 129.48 (d,  $J = 8.6$  Hz), 127.58 (s), 123.69 (s), 110.30 (s), 97.12 (s), 91.00 (s), 77.34 (s), 77.02 (s), 76.70 (s), 29.67 (s), 15.02 (s), 14.74 (s), 13.41 (s), 12.96 (s).

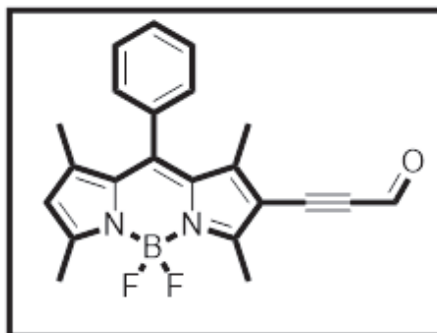


Figure 2.5. 3-(5,5-difluoro-1,3,7,9-tetramethyl-10-phenyl-5H-5 $\lambda^4$ ,6 $\lambda^4$ -dipyrrolo[1,2-c:2',1'-f][1,3,2]diazaborinin-2-yl)propionaldehyde

### 2.3.5 Synthesis of BDP-BUS

**BDP-BUS** was synthesized by using literature procedure (Zora et al., 2011). BDP-AL (40 mg, 0.10 mmol) and phenylhydrazine (11.5 mg, 0.10 mmol, 1 equiv.) in a round-bottom flask was stirred at room temperature for 5 hours. After the reaction was over, the residue was purified by column chromatography using hexane/ethyl acetate (10:1) to afford the desired product. Yield: 20 mg, 50%.  $^1\text{H}$  NMR (400 MHz,  $\text{CDCl}_3$ )  $\delta$  8.55 (s, 1H), 7.54 (dp,  $J = 6.8, 2.2$  Hz, 3H), 7.30 – 7.26 (m, 3H), 7.25 – 7.20 (m, 1H), 7.03 (ddd,  $J = 8.6, 2.3, 1.1$  Hz, 2H), 6.90 (tp,  $J = 7.4, 1.2$  Hz, 1H), 6.63 (d,  $J = 2.0$  Hz, 1H), 6.09 (s, 1H), 2.71 (s, 3H), 2.61 (s, 3H), 1.51 (s, 4H), 1.42 (d,  $J = 1.8$  Hz, 3H).  $^{13}\text{C}$  NMR (101 MHz,  $\text{CDCl}_3$ )  $\delta$  159.47 (s), 155.39 (s), 155.38 (s), 155.37 (s), 145.96 (s), 143.45 (s), 142.35 (s), 141.87 (s), 134.32 (s), 133.09 (s), 130.0 (s), 129.37 (s), 127.74 (s), 122.89 (s), 120.92 (s), 115.31 (s), 113.04 (s), 95.53 (s), 85.99 (s), 29.68 (s), 22.68 (s), 14.90 (s), 14.64 (s), 13.59 (s), 13.16 (s).

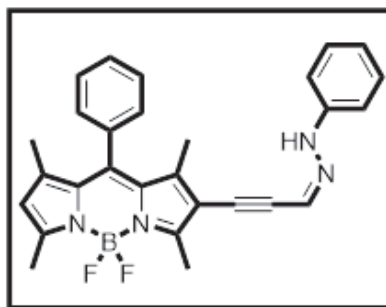


Figure 2.6. (Z)-5,5-difluoro-1,3,7,9-tetramethyl-10-phenyl-2-(3-(2 phenylhydrazono) prop-1-yn-1-yl)- 5H-5 $\lambda^4$ ,6 $\lambda^4$ -dipyrrolo[1,2-c:2',1'-f][1,3,2]diazaborinine

### 2.3.6 Synthesis of BDP-PYRZL

**BDP-PYRZL** was synthesized by using literature procedure. (Jeyaveeran et al., 2016). To a solution of BDP-BUS (20 mg, 0.042 mmol) in EtOH (2 ml) was added HgCl<sub>2</sub> (23.2 mg, 0.082 mmol, 2 equiv.) under argon and stirred at room temperature for 5 hr. After the reaction was completed, the reaction mixture was concentrated under reduced pressure and purified by column chromatography to afford the pure product of pyrazole. Yield: 10 mg, 52%. <sup>1</sup>H NMR (400 MHz, CDCl<sub>3</sub>)  $\delta$  7.68 – 7.63 (m, 1H), 7.54 – 7.43 (m, 2H), 7.36 – 7.29 (m, 5H), 7.25 (s, 1H), 7.24 – 7.19 (m, 3H), 6.06 (s, 1H), 2.57 (s, 3H), 2.18 (s, 3H), 1.40 (s, 3H), 1.13 (s, 3H). <sup>13</sup>C NMR (101 MHz, CDCl<sub>3</sub>)  $\delta$  205.64 (s), 159.08 (s), 151.58 (s), 145.80 (s), 144.49 (s), 142.47 (s), 139.83 (s), 134.38 (s), 129.51 (s), 129.27 (s), 129.02 (s), 127.76 (s), 127.58 (s), 127.52 (s), 123.48 (s), 42.69 (s), 30.92 (s), 29.68 (s), 29.30 (s), 22.68 (s), 14.85 (s), 14.62 (s), 14.14 (s), 13.15 (s), 12.81 (s).

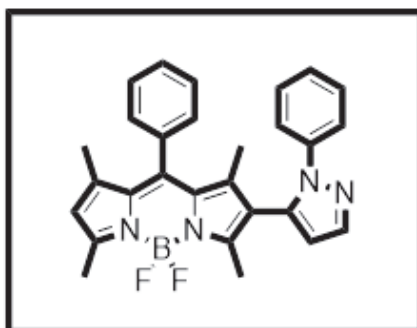


Figure 2.7. 5,5-difluoro-1,3,7,9-tetramethyl-10-phenyl-2-(1-phenyl-1H-pyrazol-5-yl)- 5H-5 $\lambda^4$ ,6 $\lambda^4$ -dipyrrolo[1,2-c:2',1'-f][1,3,2]diazaborinine

## CHAPTER 3

### RESULTS AND DISCUSSION

In this work, a new BODIPY-based fluorescent probe for the detection of mercury ions was developed. Based on previous studies, the activation of alkynes by Hg ions has long been known among chemists. However, a challenging point taken into consideration while designing the probe was the cross-affinity of other metal ions (e.g.  $\text{Au}^+$ ,  $\text{Au}^{3+}$ ,  $\text{Pb}^{2+}$ ,  $\text{Ag}^+$ ,  $\text{Cu}^{2+}$ ) which has the same chemical nature as mercury ions. With this all in mind, a novel fluorescent probe was designed which was expected to be non-emissive at first due to the deactivation via isomerization of the C=N bond, and its spectroscopic behaviors were determined. BDP-BUS was synthesized by the synthetic route and characterized using  $^1\text{H-NMR}$ ,  $^{13}\text{C-NMR}$ , and MS. For the applicability of mercury ions into the biological systems, the most suitable solvent system was determined. Among several combinations of solvent systems such as EtOH/PBS, HEPES/ $\text{CH}_3\text{CN}$ , EtOH/phosphate buffer, the maximum fluorescence intensity upon the addition of mercury ions was established in the  $\text{CH}_3\text{CN}/\text{PBS}$  (3:7, v/v, pH = 7.4) with 10  $\mu\text{M}$  dye concentration. Then, the effect of pH was surveyed in different pH values from 4 to 9 and it can be seen from the results that there was no fluorescence response in the absence of mercury ions. In addition, the maximum fluorescence emission was found to be in the pH range of 6-7 which showed that the probe can be used for imaging of mercury ions in biological systems. (Figure 3.1)

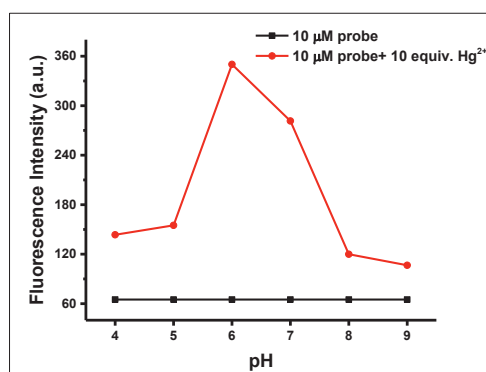


Figure 3.1. Effect of pH on the interaction of BDP-BUS (10.0  $\mu\text{M}$ ) with 10 equiv.  $\text{Hg}^{2+}$  in  $\text{CH}_3\text{CN}/\text{PBS}$  buffer solution (3:7, v/v, pH = 7.4). ( $\lambda_{\text{ex}} = 480 \text{ nm}$ ,  $\lambda_{\text{em}} = 530 \text{ nm}$  at  $25^\circ\text{C}$ )

The photophysical behavior of BDP-BUS in response to the mercury ions was assessed with the UV-Vis and fluorescence spectroscopy. The free probe showed no fluorescent emission upon excitation at 480 nm due to non-radiative deactivation process. After the addition of  $\text{Hg}^{2+}$  (10 equiv.), fluorescent emission at 530 nm and a color change from colorless to green was observed which was the result of the intramolecular cyclization over the hydrazone unit which diminished the  $\text{C}=\text{NNHR}$  isomerization (Figure 3.2.)

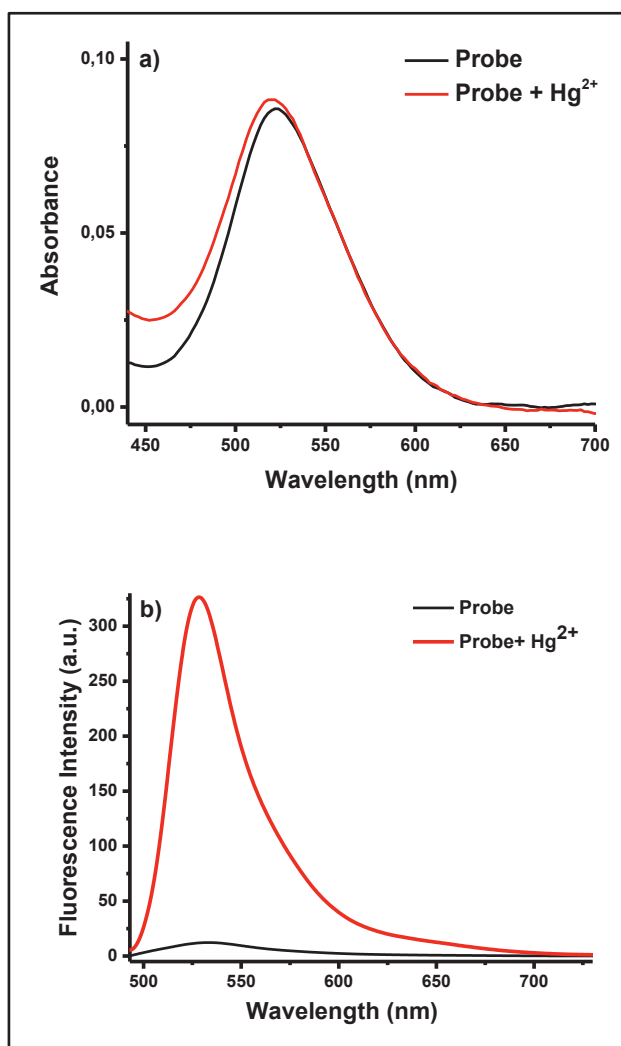


Figure 3.2. Absorption (a) and fluorescence (b) spectra of BDP-BUS (10  $\mu\text{M}$ ) in  $\text{CH}_3\text{CN}/\text{PBS}$  buffer solution (3:7, v/v, pH = 7.4) ( $\lambda_{\text{ex}} = 480 \text{ nm}$ ).

Next, the time dependency of BDP-BUS was investigated. The fluorescence intensity increased in the presence of  $\text{Hg}$  ions and became saturated within 10 minutes.

Based on this result, 10-minute standard was set for the further measurements. (Figure 3.3.)

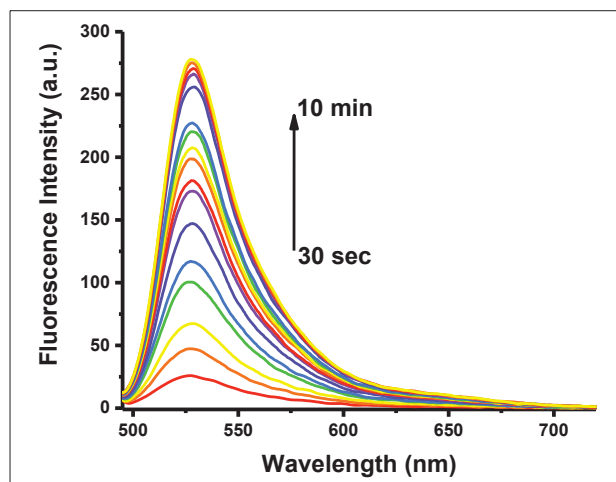


Figure 3.3. Time dependent fluorescence changes of BDP-BUS (10.0  $\mu\text{M}$ ) with 10 equiv.  $\text{Hg}^{2+}$  in  $\text{CH}_3\text{CN}/\text{PBS}$  buffer solution (3:7, v/v, pH = 7.4). ( $\lambda_{\text{ex}} = 480 \text{ nm}$ ,  $\lambda_{\text{em}} = 530 \text{ nm}$  at  $25 \text{ }^\circ\text{C}$ ) within 10 min.

Then, the fluorescent titration experiment was determined with the systematic addition of mercury ions. (Figure 3.4.) It indicated that the fluorescence intensity of BDP-BUS was dramatically increased linearly upon the addition of  $\text{Hg}^{2+}$  (0-30 equiv.) and after addition of 20 equiv. of  $\text{Hg}^{2+}$ , it became saturated and remained stable.

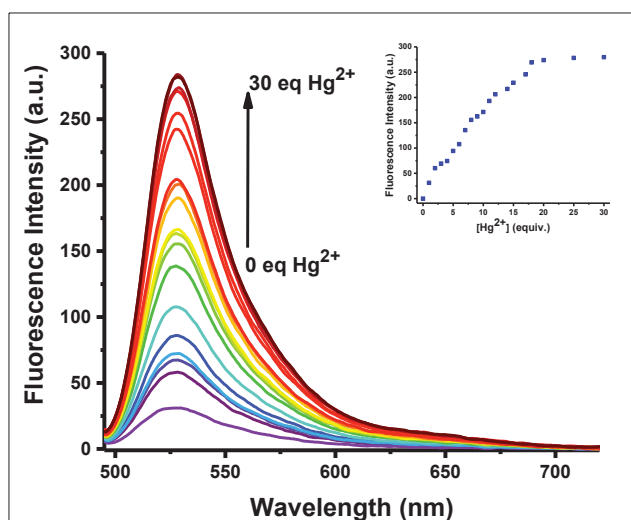


Figure 3.4. Fluorescence spectra of BDP-BUS (10  $\mu\text{M}$ ) in  $\text{CH}_3\text{CN}/\text{PBS}$  buffer solution (3:7, v/v, pH = 7.4) in the presence of different concentrations of  $\text{Hg}^{2+}$  (0–30 equiv.). Inset: Calibration curve. ( $\lambda_{\text{ex}} = 480 \text{ nm}$  at  $25 \text{ }^\circ\text{C}$ ).

Moreover, the selectivity of BDP-BUS was determined by screening its fluorescence response towards alkynophilic metal species, including  $\text{Hg}^{2+}$ ,  $\text{Au}^{3+}$ ,  $\text{Pd}^{2+}$ ,  $\text{Cu}^{2+}$ ,  $\text{Ag}^+$  and other metal species  $\text{Li}^+$ ,  $\text{Mn}^{2+}$ ,  $\text{Ca}^{2+}$ ,  $\text{Mg}^{2+}$ ,  $\text{Ba}^{2+}$ ,  $\text{Au}^+$ ,  $\text{Cr}^{2+}$ ,  $\text{Mg}^{2+}$ ,  $\text{Fe}^{3+}$ ,  $\text{Ni}^{2+}$ ,  $\text{Cu}^{2+}$ ,  $\text{Zn}^{2+}$ ,  $\text{Cd}^{2+}$  and  $\text{Al}^{3+}$  in  $\text{CH}_3\text{CN}/\text{PBS}$  buffer solution (3:7, v/v, pH = 7.4). As can be seen in Figure 3.5., the probe showed good selectivity towards  $\text{Hg}^{2+}$ . The interference of other metal in the presence of  $\text{Hg}$  ions was also determined. Therefore, BDP-BUS showed a fluorescence response to mercury ions in the presence of 50 equiv. of all other metal ions. These results proved that the probe displays excellent sensitivity and selectivity towards  $\text{Hg}^{2+}$  over other competitive ions. (Figure 3.5)

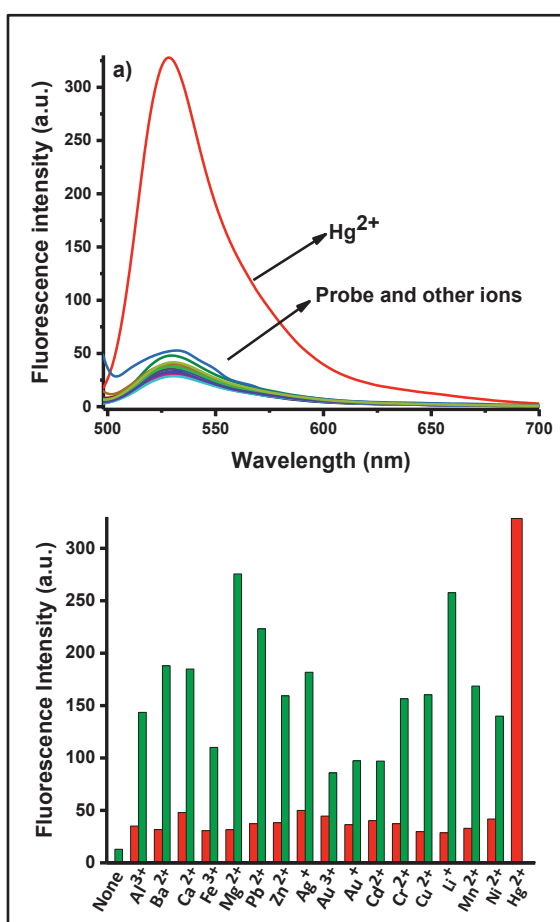


Figure 3.5. a) Fluorescence intensity of BDP-BUS (10  $\mu\text{M}$ ) in  $\text{CH}_3\text{CN}/\text{PBS}$  buffer (3:7, v/v, pH=7.4) with representative cations (100  $\mu\text{M}$ ) b) fluorescence responses of BDP-BUS to various metal ions including  $\text{Hg}^{2+}$ ,  $\text{Au}^{3+}$ ,  $\text{Pd}^{2+}$ ,  $\text{Cu}^{2+}$ ,  $\text{Ag}^+$ ,  $\text{Li}^+$ ,  $\text{Mn}^{2+}$ ,  $\text{Ca}^{2+}$ ,  $\text{Mg}^{2+}$ ,  $\text{Ba}^{2+}$ ,  $\text{Au}^+$ ,  $\text{Cr}^{2+}$ ,  $\text{Mg}^{2+}$ ,  $\text{Fe}^{3+}$ ,  $\text{Ni}^{2+}$ ,  $\text{Cu}^{2+}$ ,  $\text{Zn}^{2+}$ ,  $\text{Cd}^{2+}$  and  $\text{Al}^{3+}$ . Red bars represent the addition of 50.0 equiv. of metal ions to a 10  $\mu\text{M}$  solution of BDP-BUS ( $\text{CH}_3\text{CN}/\text{PBS}$  buffer (3:7, v/v, pH= 7.4). Green bars represent the addition of 10 equiv. of  $\text{Hg}^{2+}$  to the solutions containing BDP-BUS (10  $\mu\text{M}$ ) and the appropriate metal ions (50.0 equiv.). ( $\lambda_{\text{ex}} = 480 \text{ nm}$ ).

To determine the detection limit of BDP-BUS towards  $\text{Hg}^{2+}$ , the fluorescence titration experiment was performed. The emission intensity of the probe (10  $\mu\text{M}$ ) was measured 10 times to calculate the standard deviation of blank. A linear relationship between the fluorescence intensity and  $\text{Hg}^{2+}$  concentration was observed in the range 0 - 1  $\mu\text{M}$  ( $R^2 = 0.9541$ ). The detection limit is then calculated with the equation: detection limit =  $3\sigma_{bi}/m$ , where  $\sigma_{bi}$  is the standard deviation of blank measurements;  $m$  is the slope between intensity versus sample concentration. The detection limit was measured to be 29 nM.

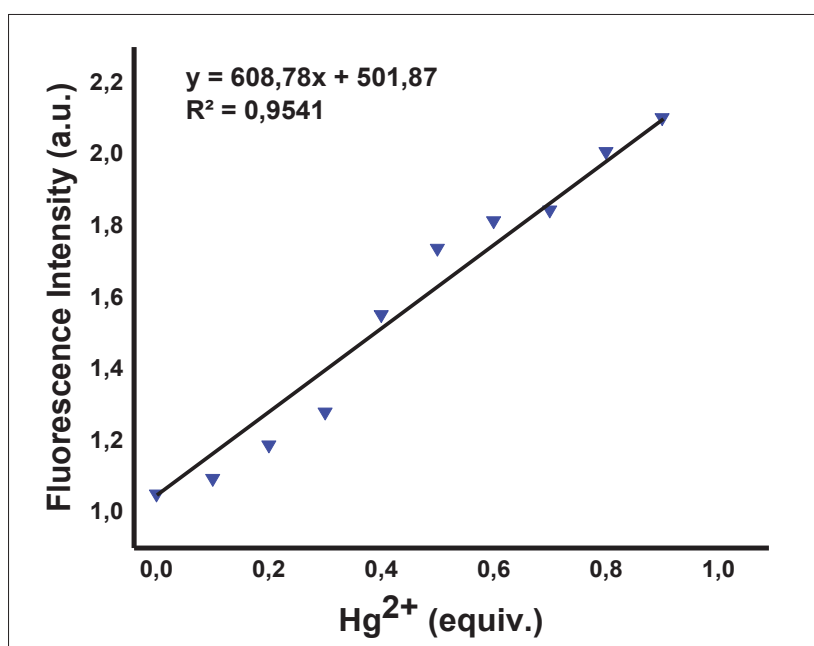


Figure 3.6. Fluorescence changes of BU-49 (10.0  $\mu\text{M}$ ) upon addition of  $\text{Hg}^{2+}$  (0.1 to 1 equiv.) in ACN/PBS buffer solution (3:7, v/v, pH = 7.4). ( $\lambda_{\text{ex}} = 480 \text{ nm}$ ,  $\lambda_{\text{em}} = 530 \text{ nm}$  at 25  $^{\circ}\text{C}$ )

As shown in Figure 3.7., the identification of  $\text{Hg}^{2+}$  was proceeded by a sequential process started with the activation of triplet bond by  $\text{Hg}^{2+}$ . Then with the addition of - NNHPh (phenylhydrazine), intermolecular cyclization promoted and produced a BODIPY derivative appended with a pyrazole ring. As a result of this process, a green emission was observed.



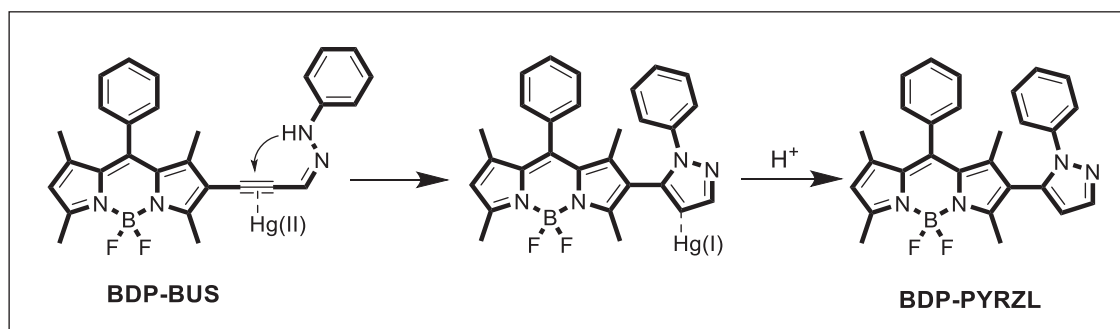


Figure 3.7. Cyclization reaction of BDP-BUS

Relying upon the promising properties of the designed probe, its sensing ability in living systems was examined. To this goal, human lung adenocarcinoma cells (A549) were incubated first with BDP-BUS (10  $\mu\text{M}$ ) for 30 min, then washed with PBS buffer three times. This process was followed by incubation with  $\text{Hg}^{2+}$  (100  $\mu\text{M}$ ) for 30 min and rinsed with PBS buffer three times. Then, the cells were stained with DAPI (1.0 mM) and the fluorescence images were obtained after 10 min. The images indicated that the cells showed a healthy spread, and no fluorescence signal was observed absence of  $\text{Hg}^{2+}$ . On the other hand, the cells incubated with  $\text{Hg}^{2+}$  exhibited a bright green fluorescence signal.

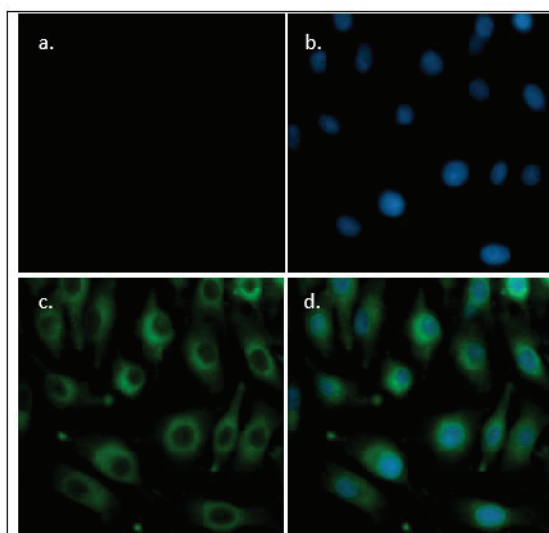


Figure 3.8. Fluorescence images of human lung adenocarcinoma (A549) cells. (a) Fluorescence image of A549 cells treated with only BDP-BUS (10  $\mu\text{M}$ ); (b) fluorescence image of cells treated with DAPI (control); (c) fluorescence image of cells treated with BDP-BUS (10  $\mu\text{M}$ ) and  $\text{Hg}^{2+}$  (100  $\mu\text{M}$ ) ( $\lambda_{\text{ex}} = 480 \text{ nm}$ ); (d) merged images of frames b- c.

## CHAPTER 4

### CONCLUSION

In this study, a new fluorescent probe derivatized with an alkyne moiety for the sensitive and selective detection of Hg ions was developed. Photophysical properties of the probe were examined and its imaging capacity for Hg<sup>2+</sup> species in living cell was also determined.

BODIPY core was used as a fluorophore and the probe showed no fluorescence emission in absence of Hg ions ( $\Phi_F= 0.09$ ) due to the deactivation via isomerization of the C=N bond. In the presence of mercury species, intramolecular cyclization over the hydrazone unit was took place and a distinct green color was observed as a result of the formation of a desired product (BDP-PYRZL) ( $\Phi_F=0.7$ ).

The probe was highly selective towards mercury species, with very low detection limit (29 nM) and there was no interference arising from other metal ions such as Ag<sup>+</sup>, Au<sup>3+</sup> and Pb<sup>2+</sup> which also have an alkynophilic nature.

Furthermore, the sensing ability of BDP-BUS in human lung adenocarcinoma (A549) cell line was investigated. The probe exhibited a high selectivity towards mercury species in living cells, providing a bright green color in existence of Hg ions.

## REFERENCES

- Atta, A.; Kim, S.; Heo, J.; Cho, D. Hg(II)-Mediated Intramolecular Cyclization Reaction In Aqueous Media And Its Application As Hg(II) Selective Indicator. *Organic Letters*. 2013, 15, 1072-1075.
- Bobileva, O.; Ikaunieks, M.; Duburs, G.; Mandrika, I.; Petrovska, R.; Klovins, J.; Loza, E. Synthesis And Evaluation Of (E)-2-(5-Phenylpent-2-En-4-Ynamido) Cyclohex-1-En-1-Carboxylate Derivatives As HCA2 Receptor Agonists. *Bioorganic & Medicinal Chemistry*. 2017, 25, 4314-4329.
- Boens, N.; Leen, V.; Dehaen, W. Fluorescent Indicators Based on Bodipy. *Chem. Soc. Rev.* 2012, 41, 1130-1172.
- Chen, J.; Burghart, A.; Derecskei-Kovacs, A.; Burgess, K. 4,4-Difluoro-4-Bora-3A,4A-Diaza-S-Indacene (BODIPY) Dyes Modified For Extended Conjugation And Restricted Bond Rotations. *The Journal of Organic Chemistry*. 2000, 65, 2900-2906.
- Culzoni, M. J.; A. De la Pena, M.; Machuca, A.; H. Goicoechea, C.; Babiano, R. Rhodamine and BODIPY Chemodosimeters and Chemosensors for The Detection of Hg<sup>2+</sup>, Based on Fluorescence Enhancement Effects. *Anal. Methods*. 2013, 5, 30-49.
- Dong, M.; Wang, Y.-W.; Peng, Y. Highly Selective Ratiometric Fluorescent Sensing For Hg<sup>2+</sup> and Au<sup>3+</sup>, Respectively, in Aqueous Solution. *Org. Lett.* 2010, 12, 5310-5313.
- Duan, X.; Gu, B.; Zhou, Q.; Hu, X.; Huang, L.; Su, W.; Li, H. A Simple Fluorescent Probe For Detecting Mercury(II) Ion In Aqueous Solution And On Agar Gels. *Journal of the Iranian Chemical Society*. 2017, 14, 1207-1214.
- Jeyaveeran, J.; Praveen, C.; Arun, Y.; M Prince, A.; Perumal, P. Cycloisomerization Of Acetylenic Oximes And Hydrazones Under Gold Catalysis: Synthesis And

- Cytotoxic Evaluation Of Isoxazoles And Pyrazoles. *Journal of Chemical Sciences*. 2015, 128, 73-83.
- Kaur, M.; Choi, D. Dual Channel Receptor Based On Diketopyrrolopyrrole Alkyne Conjugate For Detection Of Hg<sup>2+</sup>/Cu<sup>2+</sup> By “Naked Eye” And Fluorescence. *Sensors and Actuators B: Chemical* 2014, 190, 542-548.
- Lee, H.; Kim, H. –J. Ratiometric Fluorescence Chemodosimeter for Mercuric Ions Through the Hg (II)-Mediated Propargyl Amide to Oxazole Transformation. *Tetrahedron Lett.* 2011, 52, 4775–4778.
- Leen, V.; Van der Auweraer, M.; Boens, N.; Dehaen, W. Vicarious Nucleophilic Substitution Of A-Hydrogen Of BODIPY And Its Extension To Direct Ethenylation. *Organic Letters*. 2011, 13, 1470-1473.
- Li, Z.; Mintzer, E.; Bittman, R. First Synthesis of Free Cholesterol-BODIPY Conjugates. *J. Org. Chem.* 2006, 71, 1718-1721
- Lin, W.; Cao, X.; Ding, Y.; Yuan, L.; Long, L. A Highly Selective and Sensitive Fluorescent Probe for Hg<sup>2+</sup> Imaging in Live Cells Based on a Rhodamine–thioamide–alkyne Scaffold. *Chem. Commun.* 2010,46, 3529–3531.
- Loudet, A.; Burgess, K. BODIPY Dyes And Their Derivatives: Syntheses And Spectroscopic Properties. *Chemical Reviews*. 2007, 107, 4891-4932.
- Ni, Y.; Wu, J. Far-Red And Near Infrared BODIPY Dyes: Synthesis And Applications For Fluorescent Ph Probes And Bio-Imaging. *Organic & Biomolecular Chemistry*. 2014, 12, 3774.
- Panteleev, J.; Huang, R.; Lui, E.; Lautens, M. Addition Of Arylboronic Acids To Arylpropargyl Alcohols En Route To Indenes And Quinolines. *Organic Letters*. 2011, 13, 5314-5317.
- Patil, N. T.; Shinde, V. S.; Thakare, M. S.; Kumar, P. H.; Bangal, P. R.; Barui, A. K.; Patra, C. R. Exploiting the higher alkynophilicity of Au-species: development of a highly selective fluorescent probe for gold ions. *Chem. Commun.* 2012, 48, 11229–11231.

- Rasheed, T.; Bilal, M.; Nabeel, F.; Iqbal, H.; Li, C.; Zhou, Y. Fluorescent Sensor Based Models For The Detection Of Environmentally-Related Toxic Heavy Metals. *Science of The Total Environment*. 2018, 615, 476-485.
- Sauer, R.; Turshatov, A.; Balushev, S.; Landfester, K. One-Pot Production of Fluorescent Surface-Labeled Polymeric Nanoparticles via Miniemulsion Polymerization with Bodipy Surfmers. *Macromolecules*. 2012, 45, 3787–3796.
- Shah, M.; Thangaraj, K.; Soong, M.-L.; Wolford, L. T.; Boyer, J. H.; Politzer, I. R.; Pavlopoulos, T. G. Pyromethenes-BF<sub>2</sub> Complexes As Laser Dyes. *Heteroat. Chem.* 1990, 1, 389
- Song, F. L.; Watanabe, S.; Floreancig, P. E.; Koide, K. Oxidation-Resistant Fluorogenic Probe for Mercury Based on Alkyne Oxymercuration. *J. Am. Chem. Soc.* 2008, 130, 16460–16461.
- Treibs, A.; Kreuzer, F. Difluorboryl-Komplexe von Di- and Tripyrrylmethenen. *Justus Liebigs Ann. Chem.* 1968, 718, 208-223.
- Ucuncu, M.; Karakuş, E.; Emrullahoglu, M. A Ratiometric Fluorescent Probe For Gold And Mercury Ions. *Chemistry -A European Journal* 2015, 21, 13201-13205.
- Ulrich, G.; Ziessel, R.; Harriman, A. The Chemistry Of Fluorescent Bodipy Dyes: Versatility Unsurpassed. *Angewandte Chemie International Edition*. 2008, 47, 1184-1201.
- Vengaiyan, K.; Britto, C.; Sivaraman, G.; Sekar, K.; Singaravadivel, S. Phenothiazine Based Sensor For Naked-Eye Detection And Bioimaging Of Hg (II) And F<sup>-</sup> Ions. *RSC Advances*. 2015, 5, 94903-94908.
- Wood, T.; Thompson, A. Advances in the Chemistry of Dipyrrins and Their Complexes. *Chem. Rev.* 2007, 107, 1831-1861
- Wu, D.; Huang, W.; Duan, C.; Lin, Z.; Meng, Q. Highly Sensitive Fluorescent Probe For Selective Detection Of Hg<sup>2+</sup> In DMF Aqueous Media. *Inorganic Chemistry*. 2007, 46, 1538-1540.

- Wu, J.-S.; Hwang, I.-C.; Kim, K. S.; Kim, J. S. Rhodamine-Based Hg<sup>2+</sup>-Selective Chemodosimeter in Aqueous Solution: Fluorescent OFF-ON. *Org. Lett.* 2007, 9, 907–910.
- Wu, L.; Burgess, K. A New Synthesis Of Symmetric Boraindacene (BODIPY) Dyes. *Chemical Communications.* 2008, 4933.
- Wu, W.; Guo, H.; Wu, W.; Ji, S.; Zhao, J. Organic Triplet Sensitizer Library Derived from a Single Chromophore (BODIPY) with Long-Lived Triplet Excited State for Triplet–Triplet Annihilation Based Upconversion. *J. Org. Chem.* 2011, 76, 7056–7064.
- Yakubovskiy, V. P.; Shandura, M. P.; Kovtun, Y. P. Boradipyromethenecyanines. *Eur. J. Org. Chem.* 2009, 2009, 3237-3243
- Zora, M.; Kivrak, A. Synthesis Of Pyrazoles Via Cu-Mediated Electrophilic Cyclizations Of A, B-Alkynic Hydrazones. *The Journal of Organic Chemistry.* 2011, 76, 9379-9390.

## APPENDIX A

### $^1\text{H}$ -NMR AND $^{13}\text{C}$ -NMR SPECTRA OF COMPOUNDS

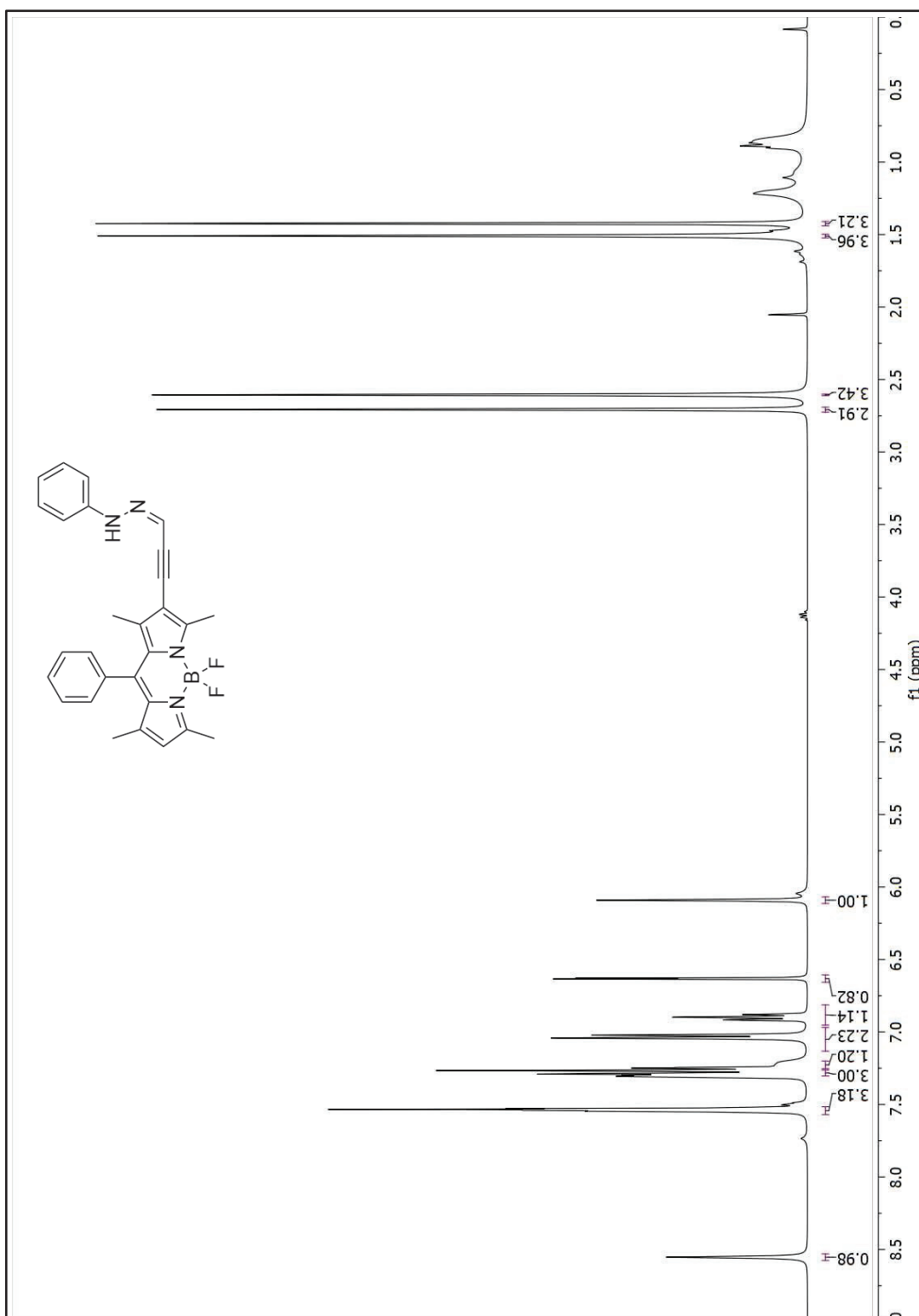


Figure A.1.  $^1\text{H}$  NMR of **BDP-BUS**

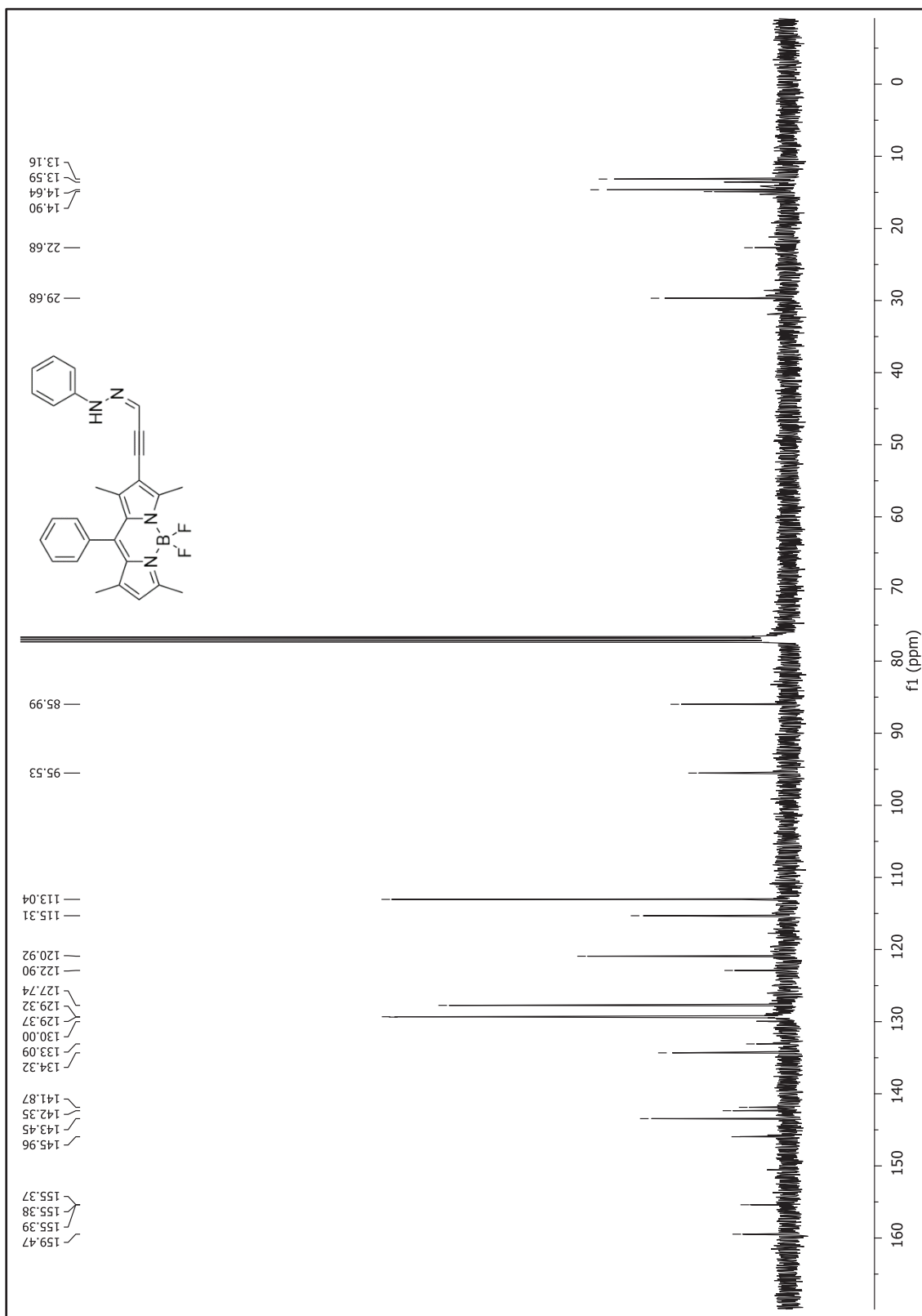


Figure A.2. <sup>13</sup>C NMR of **BDP-BUS**



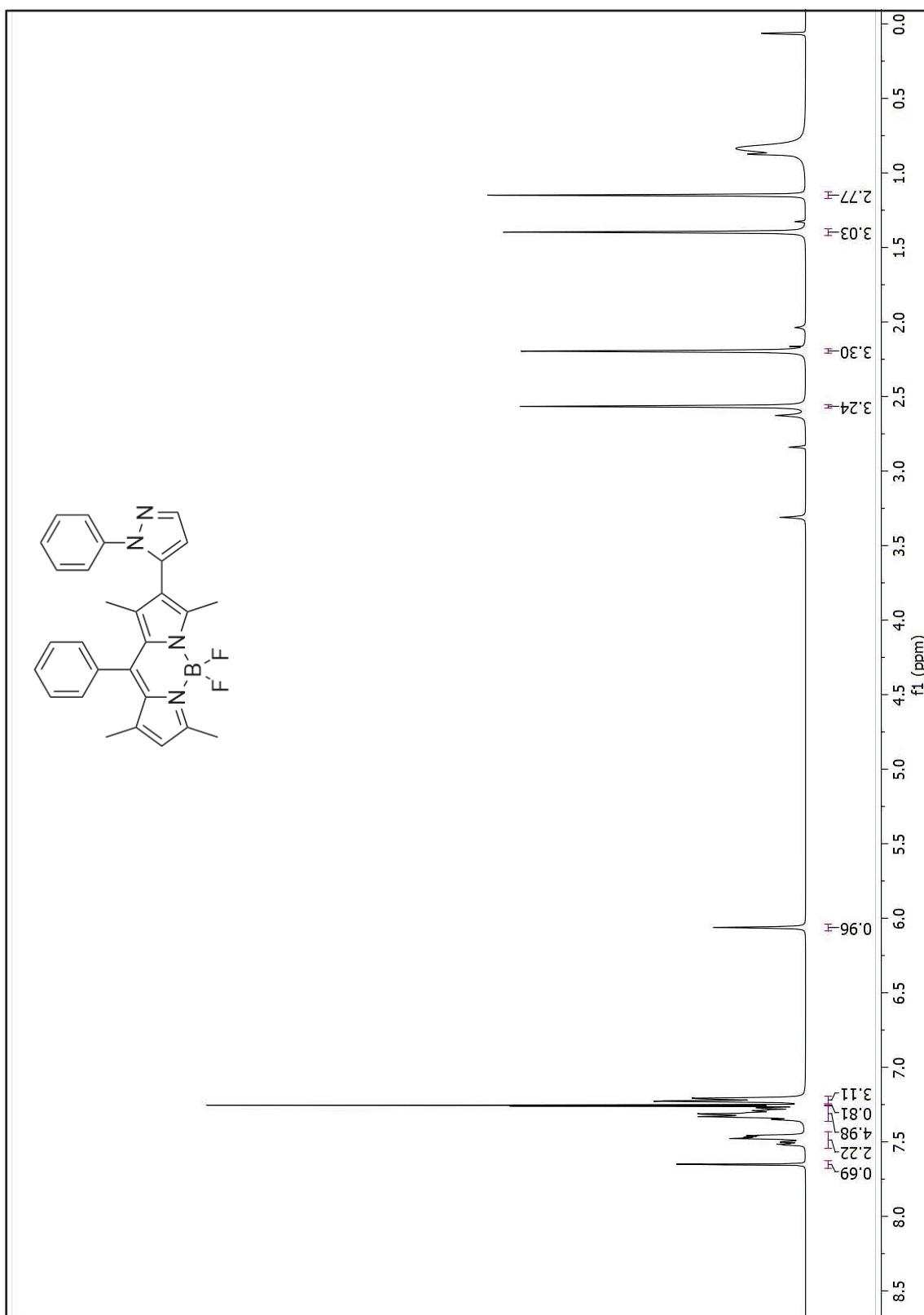


Figure A.3. <sup>1</sup>H NMR of **BDP-PYRZL**

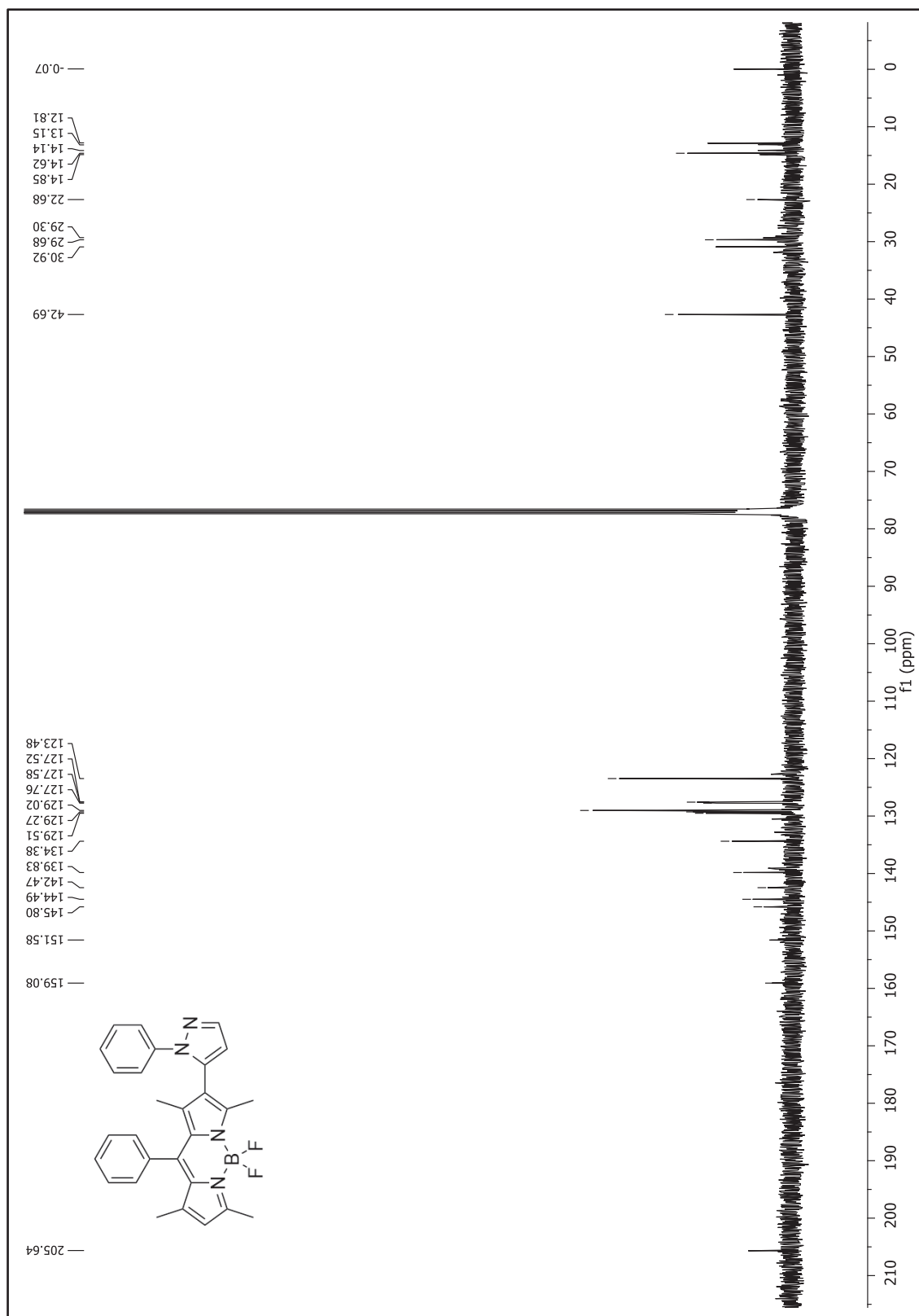


Figure A.4.  $^{13}\text{C}$  NMR of **BDP-PYRZL**

## APPENDIX B

### MASS SPECTRA OF COMPOUNDS

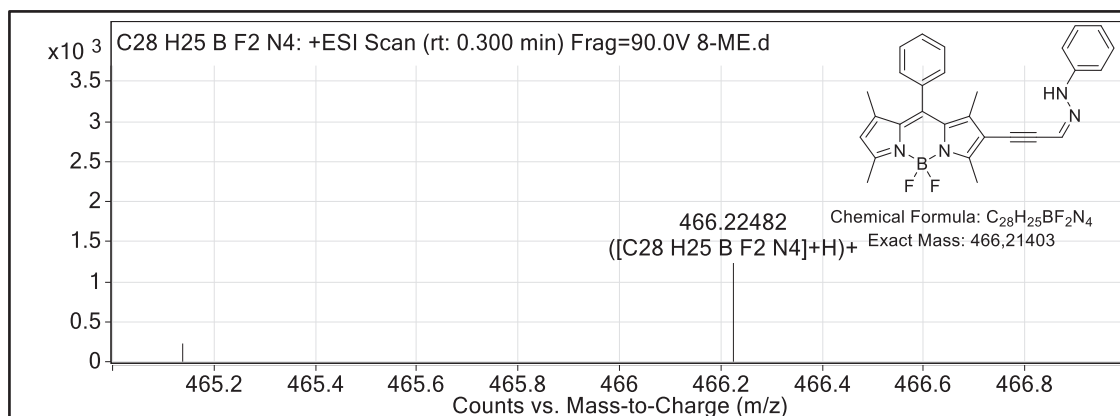


Figure B.1. Mass spectrum of **BDP-BUS** ((*Z*)-5,5-difluoro-1,3,7,9-tetramethyl-10-phenyl-2-(3-(2-phenylhydrazono)prop-1-yn-1-yl)-5*H*-5 $\lambda^4$ ,6 $\lambda^4$ -dipyrrolo [1,2-*c*:2',1'-*f*][1,3,2]diazaborinine)

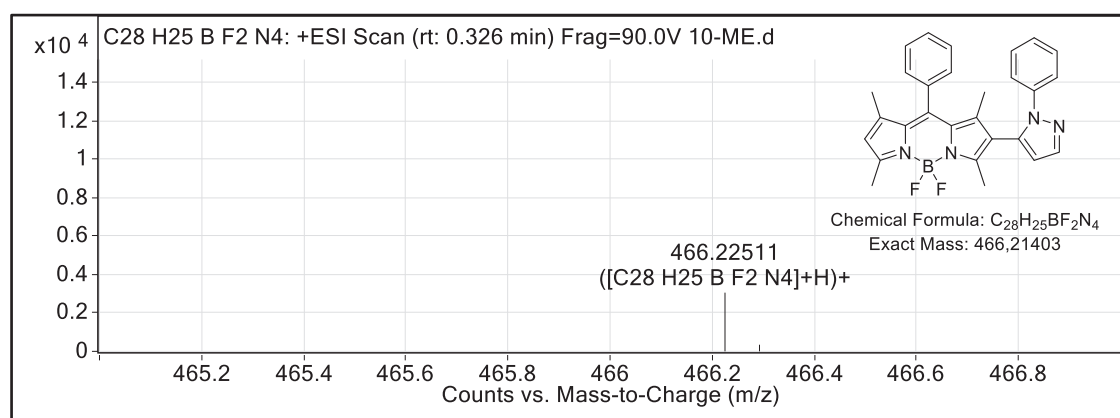


Figure B.2. Mass spectrum of **BDP-PYRZL** (5,5-difluoro-1,3,7,9-tetramethyl-10-phenyl-2-(1-phenyl-1*H*-pyrazol-5-yl)-5*H*-5 $\lambda^4$ ,6 $\lambda^4$ -dipyrrolo[1,2-*c*:2',1'-*f*][1,3,2]diazaborinine)